Both normal stem cells and CSCs largely share surface marker phenotype and molecular machinery concerning self-renewal and differentiation. These phenotypic characteristics of CSCs have been well documented in hematological malignancies [8,9], but little is shown in solid tumors including hepatocellular carcinoma (HCC). Furthermore, it is likely that CSCs are closely associated with not only carcinogenesis but also the recurrence and metastasis of tumors [10]. HCC is one of the most common malignancies worldwide and frequently shows strong resistance to traditional anticancer therapies such as chemotherapy and radiotherapy [11,12]. However, there is not sufficient evidence on CSCs in primary HCC. Thus, both the characterization and an understanding of the CSC system in liver are of paramount importance to elucidate mechanisms underlying hepatocarcinogenesis and to establish novel therapeutic approaches.

In this review, we will summarize the recent progress in CSC research in HCC and the molecular machinery underlying hepatocarcinogenesis. We also provide a perspective on therapeutic approaches against HCC from the CSC standpoint.

2. Normal hepatic stem cells

Normal adult hepatocytes are ordinarily in the quiescent G_0 state and mitotically inactive, although the liver regenerates quickly after acute injury and volume loss [13]. The regeneration is accomplished by the simple duplication of mature hepatocytes without the activation of stem/progenitor cells [14]. The presence of hepatic stem cells has been in doubt for some time. However, recent studies have successfully identified and characterized hepatic stem cells not only in fetal livers but also in adult livers (Table 1) [15,16].

2.1. Stem/progenitor cells in fetal livers

In the developing liver, both fibroblast growth factor (FGF) and bone morphogenetic protein (BMP) signals promote the commitment of ventral endoderm to the liver bud (Fig. 1) [17]. During liver bud growth, bipotent progenitors termed hepatoblasts proliferate and differentiate into hepatocytes and cholangiocytes under the control of various sets of transcription factors. Hepatoblasts could be identified as RT1A1$^-$OX18^{low}ICAM-1$^+$, Liv2$^+$, E-cadherin$^+$, Dlk1$^+$ or c-Met$^+$CD49f$^{+/low}$c-Kit$^-$CD45$^-$TER119$^-$ cells in the developing rodent liver utilizing cell sorting technology and clonal colony assays [18–23]. Interestingly, a portion of c-Met$^+$CD49f$^{+/low}$c-Kit$^-$CD45$^-$TER119$^-$ cells lack the expression of albumin, a specific marker of hepatocyte differentiation. These albumin$^-$ cells give rise to albumin$^+$ progenitor cells in response to hepatocyte growth factor (HGF) and differentiate into hepatocytes and cholangiocytes [24]. They also retain the potential to differentiate into non-hepatic lineages, pancreatic aciner cells and intestinal cells [23,24]. These findings indicate that c-Met$^+$CD49f$^{+/low}$c-Kit$^-$CD45$^-$TER119$^-$ cells include a small number of pluripotent precursors of hepatoblasts or hepatic stem cells.

In an investigation of human fetal liver, Schmelzer et al. found that epithelial cell adhesion molecule (EpCAM/CD326)$^+$ cells can be divided into two subtypes [25]; (a) hepatoblasts positive for intercellular adhesion molecule-1 (ICAM-1), alpha-fetoprotein (AFP), albumin, cytokeratin 19 (CK19) and CD133, and (b) human hepatic stem cells (hHpSCs), accounting for less than 5% of EpCAM$^+$ cells, positive for CK19, CD133, neural cell adhesion molecule (NCAM) and claudin 3, but not for ICAM-1, AFP and albumin. These populations behaved differently in colony assays and hHpSCs are assumed to be pluripotent precursors of hepatoblasts (Fig. 1).

2.2. Stem/progenitor cells in adult livers and oval cells

Although the identification of adult stem cells in normal liver has been a challenge for some time, recent studies have shown that EpCAM$^+$ liver cells purified from adult livers possess considerably similar biological characteristics to those from fetal livers and function as hepatic stem cells [25]. Given that some EpCAM$^+$ cells are also positive for CD133 and NCAM, it might be possible to further enrich

Table 1
Cell surface markers for hepatic stem/progenitor cells.

Surface markers	Source	Frequency (%)	Reference
Fetal liver			
RT1A1$^-$OX18^{low}ICAM-1$^+$	Rat (ED13)		[18]
Liv2$^+$	Mouse (ED10.5–12.5)	20–60	[19]
E-cadherin$^+$	Mouse (ED 12.5)		[20]
Dlk-1$^+$	Mouse (ED 14.5)	Nearly 10	[21]
Dlk-1$^+$	Rat (ED 14)	5.7 ± 0.9	[22]
c-Met$^+$CD49f$^{+/low}$c-Kit$^-$CD45$^-$TER119$^-$	Mouse (ED 13.5)	1.90 ± 0.33	[23]
EPCAM$^+$	Human (16–20 wk fetus)	12.1 ± 2.3	[25]
Adult liver			
EpCAM$^+$	Human (pediatric)	2.1 ± 1.6	[25]
	(adult)	1.3 ± 1.0	
Injured liver			
CD133$^+$ CD45$^-$	Mouse (DDC diet)	<0.05	[27]
Thy-1$^+$	Rat (AAF/PH or AAF/CC14)		[28]
Sca-1$^+$CD34$^+$CD45$^+$	Mouse (DDC diet)		[29]
EpCAM$^+$	Rat (AAF/PH)		[32]

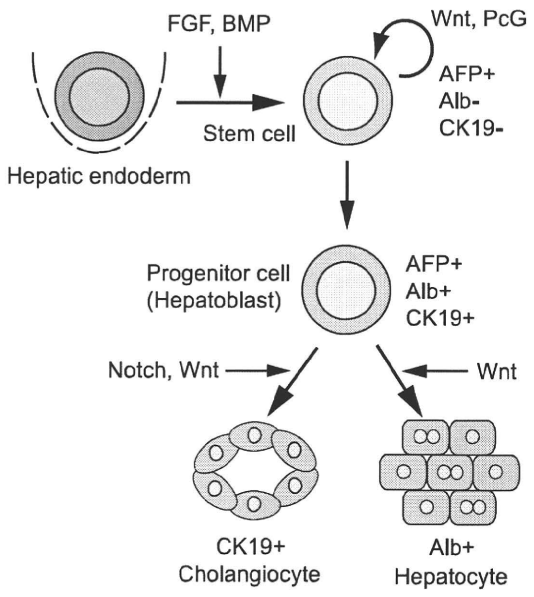

Fig. 1. Hepatogenesis and the regulatory machinery involved. In the developing liver, both fibroblast growth factor (FGF) signal from the cardiac mesoderm and bone morphogenetic protein (BMP) signal from the septum transversum mesenchyme cells promote the commitment of ventral endoderm to the liver bud. In the liver bud, hepatic stem cells generate hepatoblasts, bipotent progenitor cells which subsequently give rise to hepatocytes and cholangiocytes.

the hepatic stem cell population. Prospective assays using these cells would be beneficial to promote investigations of both normal stem cells and CSCs in liver.

Oval cells are defined as small cells with an oval nucleus and scanty cytoplasm and are considered to be progenitor cells with the ability to differentiate into hepatocytes and cholangiocytes [26,27]. They emerge from the periportal region in regenerating liver where the proliferation of mature hepatocytes is impaired. On the basis of phenotypic characteristics in common with hematopoietic stem cells (HSCs), such as the expression of cell surface markers, CD34, c-Kit, Sca-1, and Thy1, oval cells have been considered to originate from bone marrow [28,29]. However, several reports have provided evidence that hepatic oval cells originate from the liver, not from bone marrow [30,31]. Recently, Yovchev et al. reported that $EpCAM^+$ oval cells express not only epithelial markers such as AFP, CK19 and OV-1, but also mesenchymal markers such as vimentin, glypican1 and BMP7 [32]. These oval cells show decreased expression of CD34, c-Kit and NCAM. The origin of oval cells is still controversial. This could be partially due to the heterogeneity of oval cells.

Kuwahara et al. focused on the functional definition of stem/progenitor cells of hepatic origin using label-retaining cell (LRC) assays, widely utilized for the detection of somatic stem cells in many tissues and organs [33]. They conducted bromodeoxyuridine (BrdU) LRC assays in a mouse model of N-acetyl-p-aminophenol (APAP)-induced liver injury and successfully identified LRCs in the canal of Hering (proximal biliary tree), intralobular bile ducts, periductal mononuclear cells that lack hepatocytic and biliary markers, and peribiliary hepatocytes, suggesting that the liver has a multi-tiered, flexible system of regeneration rather than a single stem/progenitor cell location [33]. These findings clearly indicate the heterogeneity of hepatic stem/progenitor cells including oval cells and the need to clarify the extent to which each subset contributes to regeneration of the liver.

3. Cancer stem cells in liver

Dysregulated self-renewal capability, following oncogenic mutations, is one of the key events in the early stages of carcinogenesis [34]. It is believed that CSCs usually arise from normal stem/progenitor cells with enhanced or acquired self-renewal capability (Fig. 2). However, it remains unclear whether this hypothesis can be applied to hepatocarcinogenesis. Many attempts have been made to detect a small subset of cancer cells with the characteristics of CSCs in HCC (Table 2).

Side population (SP) cell sorting is useful for detecting CSCs in various cancer cell lines [35]. The SP phenotype is determined by the ability to efflux the dye Hoechst 33342 through an adenosine triphosphate (ATP)-binding cassette (ABC) membrane transporter [36]. Only 0.25–0.80% of Huh7 and PLC/PRF/5 HCC cells exhibits the SP phenotype. Of note, tumor initiating capacity detected in xenotransplantation assays using immunodeficient mice has been strictly confined to SP cells [37]. One thousand SP cells was enough to generate tumors in xenotransplantation, while at least 1×10^6 unsorted HCC cells were required for tumor formation, suggesting that TICs are enriched by SP cell sorting at least 1000-fold. Considering that the frequency of HCC SP cells was less than 1%, the minority cell population detected as SP cells, but not non-SP cells, might possess tumorigenic potential in these HCC cells. However, several paradoxes have been reported to this technique. C6 glioma cells contain approximately 0.4% SP cells. In serum-free medium, C6 SP cells, but not non-SP cells are responsible for the *in vivo* tumorigenesis [38]. On the other hand,

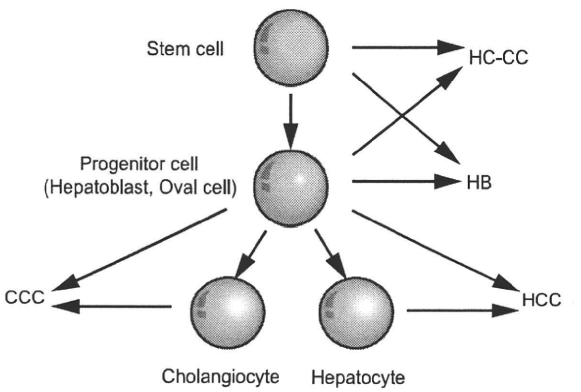

Fig. 2. Proposed model for the cellular origin of liver malignancies. Liver tumors develop from more heterogeneous cells as expected. Combined hepatocellular and cholangiocellular carcinoma (HC–CC) and hepatoblastoma (HB) are thought to be derived from primitive hepatoblasts and pluripotent stem cells. It remains unclear whether hepatocellular carcinoma (HCC) and cholangiocellular carcinoma (CCC) originate from mature cells or stem/progenitor cells.

Table 2
Cell surface markers for CSCs in HCC.

Surface markers	Frequency (HCC cell lines analyzed)	Minimal number of cells initiating tumors (cells)	Reference
Cell line			
Side population	0.25–0.80% (Huh7, PLC/PRF/5)	1×10^3	[37]
$CD133^+$	0.1–2.0% (SMMC7721)	1×10^2	[42]
$CD133^+$	8–90% (HepG2, Huh7, PLC8024, Hep3B)	1×10^3	[43]
$OV6^+$	0.2–3.0% (Huh7, SMMC7721, Hep3B, PLC, HepG2)	5×10^3	[46]
$EpCAM^+$	58.1–99.2% (Huh1, Huh7, Hep3B)	2×10^2	[47]
$CD90^+CD44^+$	0.02–2.53% (HepG2, Hep3B, PLC, Huh7, MHCC97L, MHCC97H)	5×10^2	[48]
Primary tumor			
$CD90^+CD44^+$	0.74–4.14%	2.5×10^3	[48]

most C6 cells cultured in serum-containing medium, including both SP and non-SP cells exhibit tumor initiating capacity *in vivo*, raising the possibility that C6 cells do not follow cancer stem cell theory and that non-SP cells easily suffer Hoechst toxicity and fail to grow under serum-free conditions [39,40]. The similar findings that exclude SP cell sorting technique from the major defining markers of cancer stem cells are also reported in other cancer cell types [41]. Thus, we should be more careful when applying SP cell sorting to cancer stem cell analysis including culture conditions and Hoechst cytotoxicity.

HCC cells positive for CD133, a potential cell surface marker for CSCs in a number of tumors, have been reported to exhibit greater tumorigenicity than the corresponding $CD133^-$ cells in HCC cell lines [42,43]. In mouse models of HCC, *methionine adenosyltransferase I, alpha (Mat1a)* knockout mice and *Pten* knockout mice, tumorigenic capacity was mainly detected in $CD133^+$ oval cells [44,45]. OV6 and EpCAM are also reported as specific surface markers for CSCs in HCC cell lines [46,47].

In contrast to HCC cell lines, HCC cells from surgical specimens hardly engrafted in immunodeficient mice. Recently, $CD90^+CD44^+$ cells were reported to engraft in the livers of severe combined immunodeficient (SCID)/Beige mice and behave as CSCs [48]. However, the engraftment of these cells was very inefficient and no obvious tumor masses developed. To prove that CSCs exist in human primary HCC, technical improvements to obtain better engraftment in xenotransplantation are needed. The usage of more immunodeficient mice and longer observation periods would be the approach to try first as reported [49].

4. Cell origin of liver malignancies

The cell origin of HCC has long been debated, but whether HCC originates from mature hepatocytes or stem/progenitor cells remains unclear. HCC usually develops against a setting of chronic liver injury due to chronic infection of hepatitis viruses [11]. Most well-differentiated HCCs in the early stages are detected as a small lesion with a normal level of serum AFP. Subsequently, they increase in diameter and become moderately to poorly differentiated cancerous tissues producing AFP. These findings imply that HCC might develop and progress during the de-differentiation of mature hepatocytes. On the other hand, the concept of blocked ontogeny, that maturation arrest in stem/progenitor cells contributes to cancer development, is also accepted in hepatocarcinogenesis [50]. It is evident that transformed oval cells could be a cellular origin of liver tumors [51,52]. Additionally, the activation of oval cells has been observed in not only various rodent models of carcinogenesis but also in human chronic liver disease, HCC and CCC [53,54]. Combined hepatocellular and cholangiocellular carcinoma (HC–CC) is a rare but distinct type of liver malignancy. Histological analyses revealed the proliferation of an oval-cell-like subpopulation to varying degrees except in the HCC and CC components, which indicates the role of stem/progenitor cells as the cellular origin of the tumor [55]. Consistent with this, it has been also reported that fetal liver-derived hepatic stem/progenitor cells transduced with *Bmi1* or mutant *β-catenin* acquired enhanced self-renewal capability and tumorigenicity to initiate HC–CC [56]. These observations imply that dysregulated propagation of hepatic stem/progenitor cells is an important early step in hepatocarcinogenesis. Similarly, the implantation of *p53*-null oval cells resulted in the development of HC–CC in recipient mice [57]. Therefore, HC–CC might be derived from hepatic stem/progenitor cells at least in some instances (Fig. 2).

Interestingly, it was reported that HCC could be divided into distinct subtypes sharing gene expression features with subsets of cells in differing stages of differentiation and the HCC subtypes with a similar gene expression profile to hepatic stem/progenitor cells had a poor prognosis [58,59]. Thus, HCC might develop from more heterogeneous cells during differentiation (Fig. 2).

5. Molecular machinery operating in normal and cancer stem cells in liver

Cancer-related signaling pathways, such as the Wnt, Shh, Notch and PI3K/AKT/mTOR pathways, play an important role in the maintenance or augmentation of the self-renewal capability of CSCs as well as normal stem cells (Fig. 3) [60,61]. Interestingly, however, the dependency on these signals differs somewhat between normal stem cells and CSCs [62]. Understanding the molecular mechanisms operating in normal stem cells and CSCs is essential to innovate novel therapeutic approaches.

5.1. Polycomb-group (PcG) gene products

PcG proteins are transcriptional repressors that function by modulating chromatin structure. They form chromatin-associated multiprotein complexes, polycomb repressive complex (PRC) 1 and PRC2 [63]. Bmi1, one of

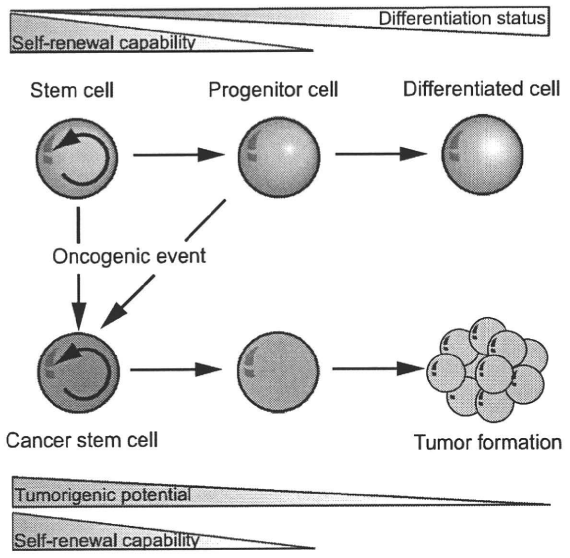

Fig. 3. Organization of cancer stem cell systems. Normal stem cells with self-renewal capability generate progenitor cells and subsequently various terminally differentiated cells. Oncogenic mutations in normal stem/progenitor cells or even in differentiated cells enhance or endow the self-renewal capability. Consequently, these cells function as cancer stem cells and contribute to the formation of bulk tumors.

the components of PRC1, regulates the cell cycle, apoptosis and senescence by repressing the *Ink4a/Arf* tumor suppressor gene locus [64]. Bmi1 is essential for the maintenance of the self-renewal capability of somatic stem cells including hepatic stem/progenitor cells [58]. On the other hand, overexpression of *Bmi1* in hepatic stem/progenitor cells augments their self-renewal capability and induces tumor development in mice [58]. Consistent with these findings, BMI1 is overexpressed in a number of tumors [65]. Of note is that it is preferentially expressed in $CD44^+$ CSCs in head and neck tumors [66] and in tumor-initiating SP cells in HCC cell lines [67]. Expression levels of BMI1 in HCC cell lines are faithfully correlated with the proportion of SP cell fraction and tumor-initiating capacity in mice [67]. Furthermore, levels of BMI1 expression in HCC were well correlated with the progression and prognosis of the disease [68]. These findings suggest that Bmi1 regulates self-renewal of both normal stem cells and CSCs by repressing the transcription of negative regulator genes for stem cell maintenance such as *Ink4a* and *Arf* [63] and by doing so, acts against oncogene-induced senescence, which is of substantial importance to the elimination of transforming cells that potentially develop into CSCs [69].

The important role of Ezh2, one of the components of PRC2, has been also recognized recently. EZH2 is also overexpressed in a variety of cancers including HCC [65]. Elucidation of its role in normal stem cells and CSCs requires further analysis.

5.2. Wnt/β-catenin signaling

Wnt/β-catenin signaling is a general regulator of self-renewal in a wide range of stem cell systems and closely associated with carcinogenesis [70]. It has been demonstrated that murine hepatic stem/progenitor cells transduced with mutant *β-catenin* acquired excessive self-renewal capability and tumorigenicity in a similar fashion to *Bmi1* [58]. In addition, Yang et al. reported that Wnt/β-catenin signaling is activated in both rodent oval cells and $OV6^+$ tumorigenic HCC cells [46]. These findings indicate that Wnt/β-catenin signaling is involved in the development and maintenance of CSCs.

Hepatoblastoma (HB) is a pediatric liver tumor. Because it shows various morphological patterns including epithelial and mesenchymal lines of differentiation, HB is considered to be derived from developmentally primitive pluripotent stem cells in some instances. Aberrant activation of Wnt/β-catenin signaling due to deletions or mutations of *β-catenin*, *adenomatous polyposis coli* (*APC*), and *Axin* is frequently observed in HBs [71]. It is reported that HBs could be divided into two subclasses, namely immature and differentiated subtypes, based on their genetic features [72]. Of interest, transcriptional programs driven by the activated Wnt/β-catenin signaling differ considerably between the two subtypes, and additional Myc activation plays an important role in the conversion of differentiated tumors into immature ones. This highlights the important role of dysregulated Wnt/β-catenin signaling in the transformation of stem/progenitor cells.

5.3. Transforming growth factor beta (TGF-β) signaling

The TGF-β/Smad signaling pathway is involved in the self-renewal and differentiation of stem cells and carcinogenesis in a variety of tissues and organs [73]. Tang et al. reported that hepatic stem/progenitor cells express TGF-β signaling-related proteins, TGF-β receptor type II (TBRII) and embryonic liver fodrin (ELF), in post-transplant human liver tissues [74]. In addition, they assumed that the activated IL-6/Stat3 pathway concomitant with the impaired TGF-β signaling in these cells is relevant to the hepatocarcinogenesis in $elf^{+/-}$ mice, which spontaneously develop HCC. This implicates the importance of TGF-β and IL-6 signaling in the CSC population in HCC.

6. Therapeutic resistance of cancer stem cells in liver

Therapeutic resistance to standard chemotherapy and radiotherapy has been attributed to CSCs in a wide spectrum of cancers [75]. Many different types of cancer cells show overexpression of ABC transporters and drug resistance genes [76]. High drug efflux capacity through ABC transporters is one of the most striking characteristics of SP cells, a rare subset of CSCs in various cancer cell lines. Consistent with this, HCC SP cells were reported to exhibit resistance to anti-cancer agents such as doxorubicin [77]. In a human acute myelogenous leukemia (AML) xenotransplantation model, leukemic stem cells (LSCs) engrafted in the bone marrow niche, where they stayed in a quiescent G_0 state. Surprisingly, up to 70% of CSCs survive cell cycle–dependent cytotoxic treatment, while LSC progenies are effectively eradicated [78]. Given the large population of HCC SP cells in G_0 phase [79], it is conceivable that CSCs in HCC also show resistance to cell cycle-specific agents.

Bao et al reported that CSCs in glioma possess an efficient DNA repair system through the activation of Chk1 and Chk2 checkpoint kinases and show resistance to irradiation therapy [80]. Although the cyclin-dependent kinase inhibitor $p21^{Waf1}$ could function as a tumor suppressor, a recent study showed that activation of $p21^{Waf1}$ is critical for DNA repair to maintain LSCs by preventing the accumulation of DNA-damage [81]. $p21^{Waf1}$ is preferentially expressed in HCC tissues rather than surrounding non-tumor tissues [82]. It is possible that well-developed DNA repair machinery operates in HCC CSCs and confers resistance to radiation therapy.

7. Therapeutic approaches for liver cancer stem cells

Although the investigation of treatments targeting CSCs in HCC has just started, strategies reported for CSCs of other tumors may offer hints for novel therapeutic approaches in HCC.

7.1. Molecular target therapy

The inhibition of CSC-specific pathways is one promising therapeutic approach. For example, LSCs of chronic myelogenous leukemia (CML) reside in the bone marrow niche in a quiescent G_0 state and are resistant to chemotherapy and targeted therapies. Nuclear protein promyelocytic leukemia protein (PML) is essential for keeping LSCs in a quiescent state. Pharmacological inhibition of PML has been shown to change LSCs sensitive to conventional and targeted therapies by recruiting them into the cell cycle [83]. Ma et al. documented that activation of the Akt/PKB and Bcl-2 pathway contributes to the chemoresistance observed in $CD133^+$ HCC cells [84]. It is noteworthy that treatment with an Akt1 inhibitor sensitized $CD133^+$ HCC cells to conventional anti-cancer drugs such as 5-FU. Aldehyde dehydrogenase (ALDH), a detoxifying enzyme which eliminates toxic byproducts of reactive oxygen species (ROS), is a marker of both normal stem cells and CSCs. It was found that ALDH is highly expressed and confers chemoresistance to alkylating agents such as cyclophosphamide in LSCs and breast CSCs [85,86]. Given that the majority of $CD133^+$ cells in HCC cell lines also show strong ALDH enzymatic activity [87], ALDH inhibitors might be effective for the eradication of CSCs in HCC.

7.2. Differentiation therapy

It is presumed that the differentiation of CSCs ultimately results in the suppression of carcinogenesis, because the tumorigenicity of CSCs is largely determined by their own self-renewal capability. It has been documented that BMPs promote the differentiation of glioma stem cells and reduce their tumorigenic potential [88]. In transgenic mice in which the expression of c-Myc is conditionally regulatable, c-Myc expression induced multiple HCCs. Upon the inactivation of Myc, HCC cells lost neoplastic properties and differentiated into hepatocytes and cholangiocytes [89]. The mice showed a decrease in tumor volume and prolonged survival. Hepatocyte nuclear factor (HNF) 4α is a central transcription factor essential for hepatogenesis [90]. A recent report showed that the gene transfer of *HNF4α* reduced a population of tumorigenic $CD90^+$ and $CD133^+$ cells purified from HCC cell lines by inducing differentiation of these subpopulations [91]. Interferon therapy is effective for not only eradicating the hepatitis viruses but also preventing the development of HCC regardless of the virological response. Interferon alpha treatment accelerated hepatocytic and biliary differentiation in oval cell lines [92]. Thus, interferon could be applied to the treatment of HCC for targeting CSCs.

7.3. Antibody therapy

Monoclonal antibody therapy is considered an important therapeutic modality for cancer. Rituximab (Anti-CD20) has already proven effective against lymphoid malignancies [93]. Although CD44, a receptor for hyaluronic acid and osteopontin, is widely expressed in both HSCs and LSCs, a monoclonal antibody specific to CD44 had a favorable effect on eradicating LSCs without affecting normal HSCs in a xenograft mouse model of human AML [94]. The administration of the CD44 antibody diminished the capacity of LSCs to home to the supportive microenvironment and promoted the terminal differentiation of LSCs *in vivo*. Given that $CD44^+$ cells function as CSCs in a variety of solid tumors including HCC [6,48], anti-CD44 antibody therapy might be a promising CSC-specific treatment in HCC.

Brain tumor stem cells reside in close proximity to blood vessels, called "vascular niches", where they receive signals that allow them to self-renew and to generate transit-amplifying cells [95]. Anti-angiogenic approaches such as the administration of anti-vascular endothelial growth factor (VEGF) monoclonal antibody disrupt vascular niches and dramatically reduce the number of CSCs. On losing the niches, CSCs cannot self-renew and differentiate into transit-amplifying cells. It is well-known that moderately to poorly differentiated HCCs are abundant in tumor vessels. Anti-angiogenic agents such as bevacizumab have already entered clinical trials for HCC and shown efficacy in some instances [96]. However, the CSC niche in HCC remains elusive. Identification of the microenvironment supportive for HCC progression is definitively needed.

8. Perspective

CSC research for HCC is somewhat behind that for other solid tumors. The major problem is that we are not sure of their existence in primary HCC. As described above, HCC cells from surgical specimens hardly engraft in conventional immunodeficient mice. This technical problem prevents us from obtaining an overall view of the CSC system in primary HCC. However, recent advances in xenotransplantation, including the co-injection of Matrigel (basement membrane matrix), usage of more immunodeficient nonobese diabetic/severe combined immunodeficiency (NOD/SCID)/interleukin-2 receptor (IL-2R) γ^{null} (NOG) mice in xenotransplantation, and longer observation periods have considerably improved the engraftment of human cancer cells. By using these approaches, approximately 25% of

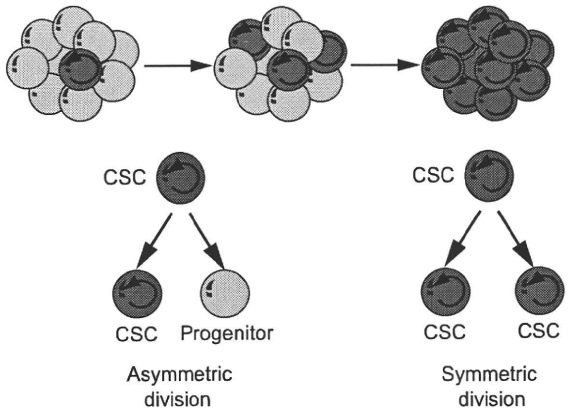

Fig. 4. Hierarchical diversity in cancer cells. Not all types of tumors have a cancer stem cell (CSC) system and CSCs do not necessarily represent a minor subpopulation of cancer cells. Asymmetrical self-renewal division of CSCs is crucial for the maintenance of a hierarchical organization in the tumor. On the contrary, predominant symmetrical self-renewal division of CSCs ultimately produces a highly homogenous population in terms of tumorigenicity as shown in melanoma cells [49].

unselected melanoma cells have been substantiated to possess tumorigenic potential [49]. Moreover, as few as 10 cells purified from murine lymphoma and AML were sufficient for the development of original hematological malignancies in syngenic transplantation assays [97]. These findings pointed out the possibility that the frequency of CSCs was underestimated in xenotransplant experiments because of a microenvironment unable to support the engraftment of donor cells. At the same time, these findings indicated that not all types of cancers fit a CSC model (Fig. 4).

Does HCC follow the CSC theory? This is a very important question. Without answering it, we cannot solve other issues, including the origin of HCC, niche for HCC, and mechanism of chemoresistance observed in HCC. Further efforts to identify and characterize HCC CSCs using improved xenotransplantation systems would provide a whole picture of the cellular organization of HCC.

9. Conflicts of interest

None declared.

Acknowledgements

The preparation of this review was supported in part by the Chiba Serum Institute Memorial Fund for Health Medical Welfare and by grants for Global Center of Excellence Program from the Ministry of Education, Culture, Sports, Science and Technology, Japan, and Core Research for Evolutional Science and Technology (CREST) of Japan Science and Technology Corporation (JST).

References

[1] P.J. Fialkow, S.M. Gartler, A. Yoshida, Clonal origin of chronic myelocytic leukemia in man, Proc. Natl. Acad. Sci. USA 58 (1967) 1468–1471.
[2] P.J. Fialkow, Use of genetic markers to study cellular origin and development of tumors in human females, Adv. Cancer Res. 15 (1972) 191–226.
[3] G.H. Heppner, Tumor heterogeneity, Cancer Res. 44 (1984) 2259–2265.
[4] T. Reya, S.J. Morrison, M.F. Clarke, I.L. Weissman, Stem cells, cancer, and cancer stem cells, Nature 414 (2001) 105–111.
[5] D.A. Shafritz, M. Oertel, A. Menthena, D. Nierhoff, M.D. Dabeva, Liver stem cells and prospects for liver reconstitution by transplanted cells, Hepatology 43 (2006) S89–98.
[6] M. Al-Hajj, M.S. Wicha, A. Benito-Hernandez, S.J. Morrison, M.F. Clarke, Prospective identification of tumorigenic breast cancer cells, Proc. Natl. Acad. Sci. USA 100 (2003) 3983–3988.
[7] C.A. O'Brien, A. Pollett, S. Gallinger, J.E. Dick, A human colon cancer cell capable of initiating tumour growth in immunodeficient mice, Nature 445 (2007) 106–110.
[8] C.H. Jamieson, I.L. Weissman, E. Passegué, Chronic versus acute myelogenous leukemia: a question of self-renewal, Cancer Cell 6 (2004) 531–533.
[9] J.C. Wang, J.E. Dick, Cancer stem cells: lessons from leukemia, Trends Cell Biol. 15 (2005) 494–501.
[10] C.T. Jordan, M.L. Guzman, M. Noble, Cancer stem cells, New Engl. J. Med. 355 (2006) 1253–1261.
[11] A.S. Befeler, A.M. Di Bisceglie, Hepatocellular carcinoma: diagnosis and treatment, Gastroenterology 122 (2002) 1609–1619.
[12] W.Y. Lau, E.C. Lai, Hepatocellular carcinoma: current management and recent advances, Hepatob. Pancreat. Dis. Int. 7 (2008) 237–257.
[13] G.K. Michalopoulos, M.C. DeFrances, Liver regeneration, Science 276 (1997) 60–66.
[14] S. Sell, Heterogeneity and plasticity of hepatocyte lineage cells, Hepatology 33 (2001) 738–750.
[15] M.H. Walkup, D.A. Gerber, Hepatic stem cells: in search of Stem cells 24 (2006) 1833–1840.
[16] L. Mishra, T. Banker, J. Murray, S. Byers, A. Thenappan, A.R. He, et al., Liver stem cells and hepatocellular carcinoma, Hepatology 49 (2009) 318–329.
[17] K.S. Zaret, M. Grompe, Generation and regeneration of cells of the liver and pancreas, Science 322 (2008) 1490–1494.
[18] H. Kubota, L.M. Reid, Clonogenic hepatoblasts, common precursors for hepatocytic and biliary lineages, are lacking classical major histocompatibility complex class I antigen, Proc. Natl. Acad. Sci. USA 97 (2000) 12132–12137.
[19] T. Watanabe, K. Nakagawa, S. Ohata, D. Kitagawa, G. Nishitai, J. Seo, et al., SEK1/MKK4-mediated SAPK/JNK signaling participates in embryonic hepatoblast proliferation via a pathway different from NF-κB-induced anti-apoptosis, Dev. Biol. 250 (2002) 332–347.
[20] M. Nitou, Y. Sugiyama, K. Ishikawa, N. Shiojiri, Purification of fetal mouse hepatoblasts by magnetic beads coated with monoclonal anti-e-cadherin antibodies and their in vitro culture, Exp. Cell Res. 279 (2002) 330–343.
[21] N. Tanimizu, M. Nishikawa, H. Saito, T. Tsujimura, A. Miyajima, Isolation of hepatoblasts based on the expression of Dlk/Pref-1, J. Cell Sci. 116 (2003) 1775–1786.
[22] M. Oertel, A. Menthena, Y.Q. Chen, B. Teisner, C.H. Jensen, D.A. Shafritz, Purification of fetal liver stem/progenitor cells containing all the repopulation potential for normal adult rat liver, Gastroenterology 134 (2008) 823–832.
[23] A. Suzuki, Y.W. Zheng, S. Kaneko, M. Onodera, K. Fukao, H. Nakauchi, et al., Clonal identification and characterization of self-renewing pluripotent stem cells in the developing liver, J. Cell Biol. 156 (2002) 173–184.
[24] A. Suzuki, A. Iwama, H. Miyashita, H. Nakauchi, H. Taniguchi, Role for growth factors and extracellular matrix in controlling differentiation of prospectively isolated hepatic stem cells, Development 130 (2003) 2513–2524.
[25] E. Schmelzer, L. Zhang, A. Bruce, E. Wauthier, J. Ludlow, H.L. Yao, et al., Human hepatic stem cells from fetal and postnatal donors, J. Exp. Med. 204 (2007) 1973–1987.
[26] E. Farber, Similarities in the sequence of early histological changes induced in the liver of the rat by ethionine, 2-acetylamino-fluorene, and 3′-methyl-4-dimethylaminoazobenzene, Cancer Res. 16 (1956) 142–149.
[27] C.B. Rountree, L. Barsky, S. Ge, J. Zhu, S. Senadheera, G.M. Crooks, A CD133-expressing murine liver oval cell population with bilineage potential, Stem Cells 25 (2007) 2419–2429.
[28] B.E. Petersen, J.P. Goff, J.S. Greenberger, G.K. Michalopoulos, Hepatic oval cells express the hematopoietic stem cell marker Thy-1 in the rat, Hepatology 27 (1998) 433–445.
[29] B.E. Petersen, B. Grossbard, H. Hatch, L. Pi, J. Deng, E.W. Scott, Mouse A6-positive hepatic oval cells also express several hematopoietic stem cell markers, Hepatology 37 (2003) 632–640.

[30] A. Menthena, N. Deb, M. Oertel, P.N. Grozdanov, J. Sandhu, S. Shah, et al., Bone marrow progenitors are not the source of expanding oval cells in injured liver, Stem Cells 22 (2004) 1049–1061.
[31] X. Wang, M. Foster, M. Al-Dhalimy, E. Lagasse, M. Finegold, M. Grompe, The origin and liver repopulating capacity of murine oval cells, Proc. Natl. Acad. Sci. USA 100 (2003) 11881–11888.
[32] M.I. Yovchev, P.N. Grozdanov, H. Zhou, H. Racherla, C. Guha, M.D. Dabeva, Identification of adult hepatic progenitor cells capable of repopulating injured rat Liver, Hepatology 47 (2008) 636–647.
[33] R. Kuwahara, A.V. Kofman, C.S. Landis, E.S. Swenson, E. Barendswaard, N.D. Theise, et al., The hepatic stem cell niche: identification by label-retaining cell assay, Hepatology 47 (2008) 1994–2002.
[34] M. Al-Hajj, M.F. Clarke, Self-renewal and solid tumor stem cells, Oncogene 23 (2004) 7274–7282.
[35] C. Wu, B. A Alman, Side population cells in human cancers, Cancer Lett. 268 (2008) 1–9.
[36] C. Hirschmann-Jax, A.E. Foster, G.G. Wulf, J.G. Nuchtern, T.W. Jax, U. Gobel, et al., A distinct "side population" of cells with high drug efflux capacity in human tumor cells, Proc. Natl. Acad. Sci. USA 101 (2004) 14228–14233.
[37] T. Chiba, K. Kita, Y.W. Zheng, O. Yokosuka, H. Saisho, A. Iwama, et al., Side population purified from hepatocellular carcinoma cells harbors cancer stem cell-like properties, Hepatology 44 (2006) 240–251.
[38] T. Kondo, T. Setoguchi, T. Taga, Persistence of a small subpopulation of cancer stem-like cells in the C6 glioma cell line, Proc. Natl. Acad. Sci. USA 101 (2004) 781–786.
[39] X. Zheng, G. Shen, X. Yang, W. Liu, Most C6 cells are cancer stem cells: evidence from clonal and population analyses, Cancer Res 67 (2007) 3691–3697.
[40] N. Platet, J.F. Mayol, F. Berger, F. Hérodin, D. Wion, Fluctuation of the SP/non-SP phenotype in the C6 glioma cell line, FEBS Lett. 581 (2007) 1435–1440.
[41] U.D. Lichtenauer, I. Shapiro, K. Geiger, M. Quinkler, M. Fassnacht, R. Nitschke, et al., Side population does not define stem cell-like cancer cells in the adrenocortical carcinoma cell line NCI h295R, Endocrinology 149 (2008) 1314–1322.
[42] S. Yin, J. Li, C. Hu, X. Chen, M. Yao, M. Yan, et al., CD133 positive hepatocellular carcinoma cells possess high capacity for tumorigenicity, Int. J. Cancer 120 (2007) 1444–1450.
[43] S. Ma, K.W. Chan, L. Hu, T.K. Lee, J.Y. Wo, I.O. Ng, et al., Identification and characterization of tumorigenic liver cancer stem/progenitor cells, Gastroenterology 132 (2007) 2542–2556.
[44] C.B. Rountree, S. Senadheera, J.M. Mato, G.M. Crooks, S.C. Lu, Expansion of liver cancer stem cells during aging in methionine adenosyltransferase 1A-deficient mice, Hepatology 47 (2008) 1288–1297.
[45] C.B. Rountree, W. Ding, L. He, B. Stiles, Expansion of CD133 expressing liver cancer stem cells in liver specific PTEN deleted mice, Stem Cells 27 (2009) 290–299.
[46] W. Yang, H.X. Yan, L. Chen, Q. Liu, Y.Q. He, L.X. Yu, et al., Wnt/beta-catenin signaling contributes to activation of normal and tumorigenic liver progenitor cells, Cancer Res. 68 (2008) 4287–4295.
[47] T. Yamashita, J. Ji, A. Budhu, M. Forgues, W. Yang, H.Y. Wang, et al., EpCAM-positive hepatocellular carcinoma cells are tumor-initiating cells with stem/progenitor cell features, Gastroenterology 136 (2009) 1012–1024.
[48] Z.F. Yang, D.W. Ho, M.N. Ng, C.K. Lau, W.C. Yu, P. Ngai, et al., Significance of CD90+ cancer stem cells in human liver cancer, Cancer Cell 13 (2008) 153–166.
[49] E. Quintana, M. Shackleton, M.S. Sabel, D.R. Fullen, T.M. Johnson, S.J. Morrison, et al., Efficient tumour formation by single human melanoma cells, Nature 456 (2008) 593–598.
[50] V.R. Potter, Phenotypic diversity in experimental hepatomas: the concept of partially blocked ontogeny. The 10th Walter Hubert Lecture, Br. J. Cancer 38 (1978) 1–23.
[51] M.L. Dumble, E.J. Croager, G.C. Yeoh, E.A. Quail, Generation and characterization of p53 null transformed hepatic progenitor cells: oval cells give rise to hepatocellular carcinoma, Carcinogenesis 23 (2002) 435–445.
[52] P. Steinberg, R. Steinbrecher, S. Radaeva, P. Schirmacher, H.P. Dienes, F. Oesch, et al., Oval cell lines OC/CDE 6 and OC/CDE 22 give rise to cholangio-cellular and undifferentiated carcinomas after transformation, Lab. Invest. 71 (1994) 700–709.
[53] K.N. Lowes, B.A. Brennan, G.C. Yeoh, J.K. Olynyk, Oval cell numbers in human chronic liver diseases are directly related to disease severity, Am. J. Pathol. 154 (1999) 537–541.
[54] T. Roskams, Liver stem cells and their implication in hepatocellular and cholangiocarcinoma, Oncogene 25 (2006) 3818–3822.
[55] N.D. Theise, J.L. Yao, K. Harada, P. Hytiroglou, B. Portmann, S.N. Thung, et al., Hepatic 'stem cell' malignancies in adults: four cases, Histopathology 43 (2003) 263–271.
[56] T. Chiba, Y.W. Zheng, K. Kita, O. Yokosuka, H. Saisho, M. Onodera, et al., Enhanced selfrenewal capability in hepatic stem/progenitor cells drives cancer initiation, Gastroenterology 133 (2007) 937–950.
[57] A. Suzuki, S. Sekiya, M. Onishi, N. Oshima, H. Kiyonari, H. Nakauchi, et al., Flow cytometric isolation and clonal identification of self-renewing bipotent hepatic progenitor cells in adult mouse liver, Hepatology 48 (2008) 1964–1978.
[58] J.S. Lee, J. Heo, L. Libbrecht, I.S. Chu, P. Kaposi-Novak, D.F. Calvisi, et al., A novel prognostic subtype of human hepatocellular carcinoma derived from hepatic progenitor cells, Nat. Med. 12 (2006) 410–416.
[59] T. Yamashita, M. Forgues, W. Wang, J.W. Kim, Q. Ye, H. Jia, et al., EpCAM and alpha-fetoprotein expression defines novel prognostic subtypes of hepatocellular carcinoma, Cancer Res. 68 (2008) 1451–1461.
[60] R. Pardal, M.F. Clarke, S.J. Morrison, Applying the principles of stem-cell biology to cancer, Nat. Rev. Cancer 3 (2003) 895–902.
[61] R. Hill, H. Wu, PTEN, stem cells, and cancer stem cells, J. Biol. Chem. 284 (2009) 11755–11759.
[62] O.H. Yilmaz, R. Valdez, B.K. Theisen, W. Guo, D.O. Ferguson, H. Wu, et al., Pten dependence distinguishes haematopoietic stem cells from leukaemia-initiating cells, Nature 441 (2006) 475–482.
[63] M.E. Valk-Lingbeek, S.W. Bruggeman, M. van Lohuizen, Stem cells and cancer; the polycomb connection, Cell 118 (2004) 409–418.
[64] I.K. Park, S.J. Morrison, M.F. Clarke, Bmi1, stem cells, and senescence regulation, J. Clin. Invest. 113 (2004) 175–179.
[65] A. Sparmann, M. van Lohuizen, Polycomb silencers control cell fate, development and cancer, Nat. Rev. Cancer 6 (2006) 846–856.
[66] M.E. Prince, R. Sivanandan, A. Kaczorowski, G.T. Wolf, M.J. Kaplan, P. Dalerba, et al., Identification of a subpopulation of cells with cancer stem cell properties in head and neck squamous cell carcinoma, Proc. Natl. Acad. Sci. USA 104 (2007) 973–978.
[67] T. Chiba, S. Miyagi, A. Saraya, R. Aoki, A. Seki, Y. Morita, et al., The polycomb gene product BMI1 contributes to the maintenance of tumor-initiating side population cells in hepatocellular carcinoma, Cancer Res. 68 (2008) 7742–7749.
[68] M. Sasaki, H. Ikeda, K. Itatsu, J. Yamaguchi, S. Sawada, H. Minato, et al., The overexpression of polycomb group proteins Bmi1 and EZH2 is associated with the progression and aggressive biological behavior of hepatocellular carcinoma, Lab. Invest. 88 (2008) 873–882.
[69] M. Collado, M.A. Blasco, M. Serrano, Cellular senescence in cancer and aging, Cell 130 (2007) 223–233.
[70] T. Reya, H. Clevers, Wnt signalling in stem cells and cancer, Nature 434 (2005) 843–850.
[71] Y. Wei, M. Fabre, S. Branchereau, F. Gauthier, G. Perilongo, M.A. Buendia, et al., Activation of beta-catenin in epithelial and mesenchymal hepatoblastomas, Oncogene 19 (2000) 498–504.
[72] S. Cairo, C. Armengol, A. De Reyniès, Y. Wei, E. Thomas, C.A. Renard, et al., Hepatic stem-like phenotype and interplay of Wnt/beta-catenin and Myc signaling in aggressive childhood liver cancer, Cancer Cell 14 (2008) 471–484.
[73] L. Mishra, K. Shetty, Y. Tang, A. Stuart, S.W. Byers, The role of TGF-beta and Wnt signaling in gastrointestinal stem cells and cancer, Oncogene 24 (2005) 5775–5789.
[74] Y. Tang, K. Kitisin, W. Jogunoori, C. Li, C.X. Deng, S.C. Mueller, et al., Progenitor/stem cells give rise to liver cancer due to aberrant TGF-beta and IL-6 signaling, Proc. Natl. Acad. Sci. USA 105 (2008) 2445–2450.
[75] J.E. Visvader, G.J. Lindeman, Cancer stem cells in solid tumours: accumulating evidence and unresolved questions, Nat. Rev. Cancer 8 (2008) 755–768.
[76] C.F. Higgins, Multiple molecular mechanisms for multidrug resistance transporters, Nature 446 (2007) 749–757.
[77] N. Haraguchi, T. Utsunomiya, Inoue H, F. Tanaka, K. Mimori, G.F. Barnard, et al., Characterization of a side population of cancer cells from human gastrointestinal system, Stem Cells 24 (2006) 506–513.
[78] F. Ishikawa, S. Yoshida, Y. Saito, A. Hijikata, H. Kitamura, S. Tanaka, et al., Chemotherapy-resistant human AML stem cells home to and engraft within the bone-marrow endosteal region, Nat. Biotechnol. 25 (2007) 1315–1321.
[79] Y. Kamohara, N. Haraguchi, K. Mimori, F. Tanaka, H. Inoue, M. Mori, et al., The search for cancer stem cells in hepatocellular carcinoma, Surgery 144 (2008) 144 119–124.

[80] S. Bao, Q. Wu, R.E. McLendon, Y. Hao, Q. Shi, A.B. Hjelmeland, et al., Glioma stem cells promote radioresistance by preferential activation of the DNA damage response, Nature 444 (2006) 756–760.
[81] A. Viale, F. De Franco, A. Orleth, V. Cambiaghi, V. Giuliani, D. Bossi, et al., Cell-cycle restriction limits DNA damage and maintains self-renewal of leukaemia stem cells, Nature 457 (2009) 51–56.
[82] L.F. Qin, I.O. Ng, S.T. Fan, M. Ng, p21/WAF1, p53 and PCNA expression and p53 mutation status in hepatocellular carcinoma, Int. J. Cancer 79 (1998) 424–428.
[83] K. Ito, R. Bernardi, A. Morotti, S. Matsuoka, G. Saglio, Y. Ikeda, et al., PML targeting eradicates quiescent leukaemia-initiating cells, Nature 453 (2008) 1072–1078.
[84] S. Ma, T.K. Lee, B.J. Zheng, K.W. Chan, X.Y. Guan, CD133+ HCC cancer stem cells confer chemoresistance by preferential expression of the Akt/PKB survival pathway, Oncogene 27 (2008) 1749–1758.
[85] S. Ma, T.K. Lee, B.J. Zheng, K.W. Chan, X.Y. Guan, Characterization of cells with a high aldehyde dehydrogenase activity from cord blood and acute myeloid leukemia samples, Stem Cells 23 (2005) 752–760.
[86] C. Ginestier, M.H. Hur, E. Charafe-Jauffret, F. Monville, J. Dutcher, M. Brown, et al., ALDH1 is a marker of normal and malignant human mammary stem cells and a predictor of poor clinical outcome, Cell Stem Cell 1 (2007) 555–567.
[87] S. Ma, K.W. Chan, T.K. Lee, K.H. Tang, J.Y. Wo, B.J. Zheng, et al., Aldehyde dehydrogenase discriminates the CD133 liver cancer stem cell populations, Mol. Cancer Res. 6 (2008) 1146–1153.
[88] S.G. Piccirillo, B.A. Reynolds, N. Zanetti, G. Lamorte, E. Binda, G. Broggi, et al., Bone morphogenetic proteins inhibit the tumorigenic potential of human brain tumour-initiating cells, Nature 444 (2006) 761–765.
[89] C.M. Shachaf, A.M. Kopelman, C. Arvanitis, A. Karlsson, S. Beer, S. Mandl, et al., MYC inactivation uncovers pluripotent differentiation and tumour dormancy in hepatocellular cancer, Nature 431 (2004) 1112–1117.
[90] F. Parviz, C. Matullo, W.D. Garrison, L. Savatski, J.W. Adamson, G. Ning, et al., Hepatocyte nuclear factor 4alpha controls the development of a hepatic epithelium and liver morphogenesis, Nat. Genet. 34 (2003) 292–296.
[91] C. Yin, Y. Lin, X. Zhang, Y.X. Chen, X. Zeng, H.Y. Yue, et al., Differentiation therapy of hepatocellular carcinoma in mice with recombinant adenovirus carrying hepatocyte nuclear factor-4alpha gene, Hepatology 48 (2008) 1528–1539.
[92] R. Lim, B. Knight, K. Patel, J.G. McHutchison, G.C. Yeoh, J.K. Olynyk, Antiproliferative effects of interferon alpha on hepatic progenitor cells in vitro and in vivo, Hepatology 43 (2006) 1074–1083.
[93] B.D. Cheson, J.P. Leonard, Monoclonal antibody therapy for B-cell non-Hodgkin's lymphoma, New Engl. J. Med. 359 (2008) 613–626.
[94] L. Jin, K.J. Hope, Q. Zhai, F. Smadja-Joffe, J.E. Dick, Targeting of CD44 eradicates human acute myeloid leukemic stem cells, Nat. Med. 12 (2006) 1167–1174.
[95] C. Calabrese, H. Poppleton, M. Kocak, T.L. Hogg, C. Fuller, B. Hamner, et al., A perivascular niche for brain tumor stem cells, Cancer Cell 11 (2007) 69–82.
[96] M.B. Thomas, J.S. Morris, R. Chadha, M. Iwasaki, H. Kaur, E. Lin, et al., Phase II trial of the combination of bevacizumab and erlotinib in patients who have advanced hepatocellular carcinoma, J. Clin. Oncol. 27 (2009) 843–850.
[97] P.N. Kelly, A. Dakic, J.M. Adams, S.L. Nutt, A. Strasser, et al., Tumor growth need not be driven by rare cancer stem cells, Science 317 (2007) 337.

Therapeutic effect of balloon-occluded retrograde transvenous obliteration for gastric varices in relation to haemodynamics in the short gastric vein

[1]H OKUGAWA, MD, [1]H MARUYAMA, MD, [1]S KOBAYASHI, MD, [1]H YOSHIZUMI, MD, [2]S MATSUTANI, MD and [1]O YOKOSUKA, MD

[1]*Department of Medicine and Clinical Oncology, Chiba University Graduate School of Medicine, 1-8-1, Inohana, Chuou-ku, Chiba, 260-8670 and* [2]*Chiba College of Health Science, 2-10-1, Wakaba, Mihama-ku, Chiba 261-0014, Japan*

ABSTRACT. The aim of this study was to elucidate the relationship between the therapeutic effect of balloon-occluded retrograde transvenous obliteration (B-RTO) and haemodynamic features in the short gastric vein (SGV) in patients with gastric fundal varices (GV). The subjects in this retrospective cohort study comprised 34 patients who had moderate- or large-grade GV with the SGV both on retrograde venography and Doppler ultrasound. The diameter, flow velocity and flow volume in the SGV measured by Doppler ultrasound before B-RTO with 1 h balloon occlusion were compared with the therapeutic effect. Embolisation of GV was achieved in 30/34 patients (88.2%): 27 by initial B-RTO and 3 by second B-RTO. Flow velocity and flow volume in the SGV before B-RTO were significantly lower in the 27 patients with a complete effect on initial B-RTO (7.19 ± 2.44 cm s^{-1}, $p=0.0246$; 189.52 ± 167.66 ml min^{-1}, $p=0.002$) than in the 7 patients with an incomplete effect (10.41 ± 5.44 cm s^{-1}, 492.14 ± 344.94 ml min^{-1}). Neither endoscopy nor contrast-enhanced CT had recurrent findings of GV in the subject during the follow-up period (94–1440 days; mean, 487.2 ± 480.5 days). In conclusion, haemodynamic evaluation of the SGV using Doppler ultrasound may be useful for the prediction of the therapeutic effect of B-RTO.

Received 16 November 2008
Revised 31 January 2009
Accepted 3 February 2009

DOI: 10.1259/bjr/28956799

Gastric varices are one of the haemodynamic features of major potential consequence in patients with portal hypertension. The incidence of gastric varices is reported to be approximately 20–25% [1–3], which is lower than that of oesophageal varices (EV). Furthermore, lower bleeding rates of gastric varices than those of EV have been described in previous studies [1, 4]. However, those studies have shown that the mortality rate caused by bleeding from gastric fundal varices (GV) is in the range of 25–55% [1–5]. Therefore, management of bleeding GV is vital in the clinical practice of patients with portal hypertension.

In 1991, Kanagawa et al [6] introduced a new technique — balloon-occluded retrograde transvenous obliteration (B-RTO) — for the treatment of GV. It is a simple and effective procedure for the embolisation of GV, and previous studies reported the complete eradication of GV in over 78% of patients, with a low rate of recurrence [6–9]. However, this technique does have some intractable cases, reportedly 12.5–40% [6, 8–10], the reason for which has not been fully discussed. High-flow volume in the GV may account for the incomplete effect of B-RTO.

It was reported that over 50% of GV have short gastric vein (SGV) and/or posterior gastric vein (PGV) dominant, and about 25% of GV have left gastric vein (LGV) dominant, blood supply on portograms [11], and that Doppler ultrasound could evaluate the haemodynamics in these gastric veins [12, 13]. As the SGV is one of the major inflow routes for GV, its haemodynamics might be related to the pathophysiology of GV and the therapeutic effect of GV after B-RTO. Based on this hypothesis, we examined the haemodynamics in the SGV using Doppler ultrasound before B-RTO. The purpose of the present study was to elucidate the relationship between the therapeutic effect of B-RTO for GV and the haemodynamic features in the SGV.

Methods and materials

Patients

83 consecutive patients (36 female, 47 male; age range, 42–80 years; mean, 62.6 ± 9.42 years) with GV were treated with B-RTO between March 1998 and September 2006 in our department. Among them, 34 patients (14 female, 20 male; age range, 46–80 years; mean, 63.6 ± 8.95 years) were enrolled in this retrospective cohort study, according to both of the following two criteria: (i) the SGV was demonstrated by retrograde venography via GV (56/83, 67.5%); (ii) detection and blood flow measurement in the SGV was conducted by Doppler ultrasound in patients who had SGV on the venogram (34/56, 60.7%). Informed written consent for B-

Address correspondence to: Hitoshi Maruyama, Department of Medicine and Clinical Oncology, Chiba University Graduate School of Medicine, 1-8-1, Inohana, Chuou-ku, Chiba 260-8670, Japan. E-mail: maru-cib@umin.ac.jp

Table 1. Clinical background of patients treated by B-RTO (n=34)

Sex (male/female)	20/14
Age (years): mean ± SD (range)	63.6±8.95 (46–80)
Application electively/prophylactically	17/17
Liver disease	
LC	33
Alcohol	8
HCV	17
HBV	2
Primary biliary cirrhosis	1
Cryptogenic	5
Chronic hepatitis	1
Cryptogenic	1
Child–Pugh class A/B	18/15
Presence of hepatocellular carcinoma	13
Form of gastric varices F1/F2/F3	0/25/9
Presence of oesophageal varices before B-RTO	17
Form of oesophageal varices F1/F2/F3	11/5/1

B-RTO, balloon-occluded retrograde transvenous obliteration; SD, standard deviation; LC, liver cirrhosis; F1, small straight; F2, enlarged tortuous; F3, large coil-shaped; HBV, hepatitis B virus; HCV, hepatitis C virus.

RTO was obtained from all patients, and the research was carried out in accordance with the Helsinki Declaration. The ethics committee in our hospital deemed this retrospective study as appropriate for publication.

33 patients had liver cirrhosis and one had chronic hepatitis. Diagnosis of liver cirrhosis was based on imaging modalities with laboratory data and clinical presentation, and diagnosis of chronic hepatitis was based on percutaneous liver biopsy. The cause of liver diseases was hepatitis B virus infection in 2 patients, hepatitis C virus infection in 17, alcohol abuse in 8, primary biliary cirrhosis in 1, and cryptogenic in 6. Hepatic functional reserve in cirrhotic patients according to the Child–Pugh classification was A in 18 patients and B in 15 patients [14]. 13 patients had hepatocellular carcinoma (HCC), which was controlled by non-surgical treatment, and none had portal venous tumour thrombus or portal venous thrombus (Table 1).

Endoscopy

GV were diagnosed by endoscopic examination in all patients. The form of GV was evaluated according to the general rules of the Japanese Society for Portal Hypertension [15]: small straight (mild grade, F1); enlarged tortuous (moderate grade, F2); or large coil-shaped (large grade, F3). 25 patients had F2 and 9 had F3. 17 of the 34 patients had bleeding histories that were confirmed by endoscopic examination: 10 with active bleeding on endoscopic findings and 7 with a bleeding history, having inactive bleeding with no other cause for gastrointestinal bleeding. 10 patients with active bleeding received endoscopic treatment to attain haemostasis before B-RTO: endoscopic variceal ligation (EVL) in 1 patient; endoscopic cyanoacrylate injection in 7 patients; both EVL and endoscopic cyanoacrylate injection in 1 patient; and endoscopic clipping following cyanoacrylate injection in 1 patient. The remaining 17 patients had no bleeding history, haematemesis or melena during their clinical course.

17 patients also had EV: 11 with F1, 5 with F2 and 1 with F3. A prophylactic treatment for EV was performed in one patient with F2 varices before B-RTO and one patient with F1 varices after B-RTO. Follow-up endoscopy was performed approximately every 6 months after B-RTO.

B-RTO

The application of B-RTO in our study constituted elective treatment in 17 patients ("bleeders") and prophylactic treatment in 17 patients who wished to receive it. All patients had a gastrorenal shunt placed for the drainage pathway from the GV by ultrasound/CT [16]. Initially, a 6F balloon catheter (Selecon MP catheter; Clinical Supply, Gifu, Japan) was inserted into the drainage route of the GV (a gastrorenal shunt). Then, retrograde venography was performed under balloon inflation to confirm the demonstration of both the GV and the inflow routes. Subsequently, the sclerosing agent prepared with equal amounts of 10% ethanolamine oleate (Oldamin; Mochida Pharmaceutical, Tokyo, Japan) and iopamidol (Iopamiron 300; Nihon Schering, Osaka, Japan) was injected in a retrograde manner under fluoroscopy to fill both the GV and the inflow routes. After ~1 h, as much of the agent as possible was withdrawn and the balloon catheter was removed. Blood pressure, pulse rate, electrocardiogram, arterial oxygen saturation and urine volume were monitored during the treatment, and 4000 units of haptoglobin (Green Cross, Osaka, Japan) was administered intravenously to prevent renal failure potentially induced by ethanolamine oleate. The therapeutic effect was evaluated by contrast-enhanced CT within 1 week after B-RTO, and therapeutic success was defined as absence of contrast enhancement in the GV on CT images. B-RTO was performed 1 week or 2 weeks after the previous B-RTO in cases of an incomplete embolisation effect in the GV. All B-RTO procedures were performed by H.M. and H.O.

Doppler ultrasound examination

Doppler ultrasound was performed using SSA-390A or SSA-770A systems (Toshiba, Tokyo, Japan) with a

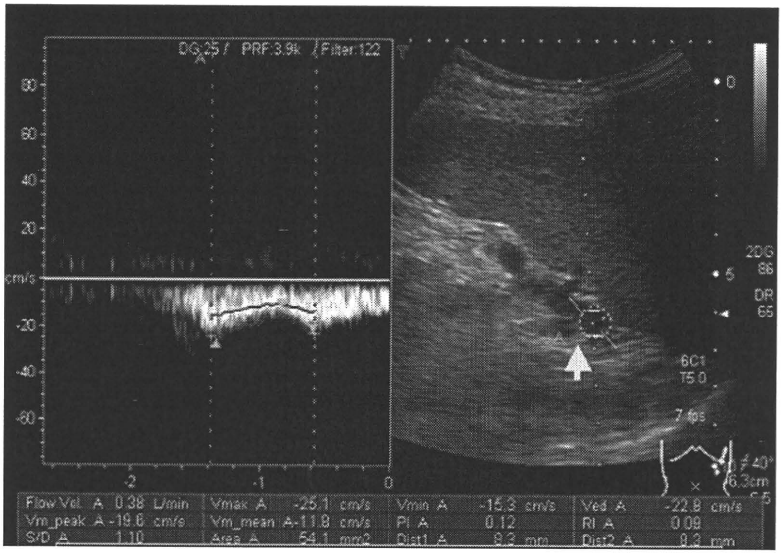

Figure 1. Doppler ultrasound of patients with gastric fundal varices. The sonogram under the left intercostal scan demonstrated the short gastric vein (SGV) with flow in the hepatofugal direction (arrow).

3.75 MHz convex probe before B-RTO. All patients underwent ultrasound examinations, after an overnight fast except for the bleeding cases, in the supine position and in an intermediate or light inspiratory phase of respiration. Among the 10 patients who received endoscopic treatments to attain haemostasis, Doppler ultrasound examination was applied emergently just before the endoscopic treatments in five bleeders and after the endoscopic treatment in the other five bleeders. The SGV was demonstrated by a left inter- or sub-costal scan around the splenic hilum (Figure 1) [12]. The beam–vessel angle was less than 60° in every patient, and the diameter (mm), flow velocity (cm s^{-1}) and mean flow volume (ml min^{-1}) of the SGV were measured by grey-scale ultrasound and the pulsed Doppler method. Doppler ultrasound was performed by H.M. (n=25) or S.M. (n=9), who were hepatologists with over 8 years of experience of ultrasound examinations at the time of the initial case. Observer variability was obtained in 12 patients by independent measurements strictly performed by two operators for interobserver variability and by one operator for intraobserver variability on the same day. The average value was used for SGV data in these 12 cases. All of the ultrasound images for the SGV were carefully reviewed by H.O. to confirm that the fast Fourier transform analysis was conducted under appropriate measurement conditions.

Contrast-enhanced CT

Contrast-enhanced CT with dynamic study was performed using Vertex 3000 Formula (GE Yokogawa Medical Systems, Hino, Japan) or Lightspeed ultra16 (GE Yokogawa Medical Systems) equipment. Iodinated contrast medium (Iopamiron 300; Nihon Schering, Osaka, Japan) was injected at 3 ml s^{-1} with a total dose of 100 ml from the antecubital vein by mechanical power injector, and scanning was performed with a 30 s delay between contrast medium administration and the start of imaging for the hepatic artery-dominant phase, a 80 s delay for the portal vein-dominant phase, and a 180 s delay for the equilibrium phase. Contrast-enhanced CT was performed before B-RTO, within 1 week after the treatment and approximately every 6 months during follow-up observation. The therapeutic effect was assessed by S.K. as the presence or absence of the contrast-enhanced findings at the variceal area.

Statistical analysis

The results in this study were expressed as mean ± standard deviation (SD). Statistical analysis was performed by Stat View-J 5.0 statistical software (Abacus Concepts, Berkeley, CA). The relationship between the therapeutic effect of B-RTO and the haemodynamics in the SGV was analysed using the Student's t-test. The interobserver or intraobserver variability was obtained as a coefficient of variation, calculated by dividing the standard deviation by the mean and multiplying by 100. p-values <0.05 were considered to be statistically significant.

Results

Embolisation effect of B-RTO

Initial B-RTO completely embolised GV in 27 of the 34 patients (79.4%), with the other 7 showing an incomplete effect. Three of the seven patients had complete embolisation effects after a second B-RTO, and another one had complete embolisation after a third B-RTO combined with percutaneous transhepatic obliteration. No additional treatment was added for the remaining three patients who declined further intervention. Therefore, B-RTO achieved an embolisation effect in 30 of the 34 patients (88.2%). 6 months after B-RTO, endoscopy showed a disappearance or decrease in size of the GV, and contrast-enhanced CT did not show any enhancement at the variceal site. Subsequently, neither endoscopy nor contrast-enhanced CT showed recurrent findings of GV in the subject during the follow-up period (94–1440 days; mean, 487.2±480.5 days). Fever (>37.5℃; 21/34 patients, 61.8%), haemoglobinuria

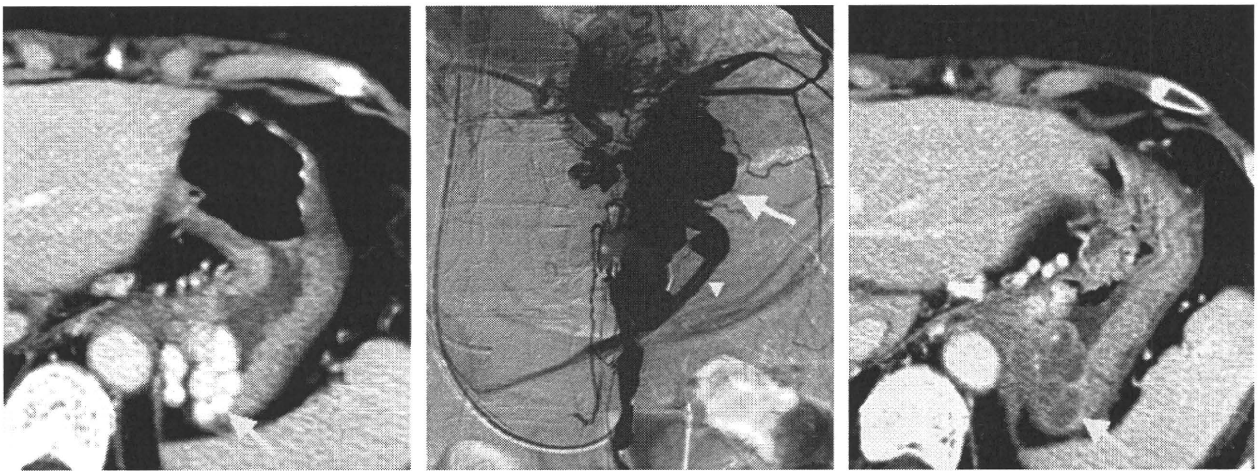

(a) (b) (c)

Figure 2. Gastric fundal varices (GV) before and after balloon-occluded retrograde transvenous obliteration (B-RTO) in a 72-year-old woman with chronic hepatitis (cryptogenic). (a) Contrast-enhanced CT before B-RTO showing the GV (arrow); (b) retrograde venography from a gastrorenal shunt showing the GV (arrow) and short gastric vein (SGV; arrowhead); (c) contrast-enhanced CT after B-RTO (contrast enhancement was not observed at the variceal site (arrow)). This case was completely treated by the initial B-RTO. Diameter, flow velocity and flow volume of the SGV on Doppler ultrasound were 6.9 mm, 6.3 cm s^{-1} and 140 ml min^{-1}, respectively.

(27/34, 79.4%) and pain (13/34, 38.2%) were found as short-term complications.

Haemodynamics of the SGV before B-RTO in relation to the therapeutic effect

The SGV had hepatofugal flow direction on Doppler sonograms in all patients before B-RTO. Flow velocity and flow volume in the vessel before B-RTO were significantly lower in the 27 patients who were completely treated by the initial B-RTO (7.19 ± 2.44 cm s^{-1}, $p=0.0246$; 189.52 ± 167.66 ml min^{-1}, $p=0.002$; Figure 2) than in the 7 patients who required two or three sessions (10.41 ± 5.44 cm s^{-1}, 492.14 ± 344.94 ml min^{-1}). The diameter of the SGV was smaller in the former (6.46 ± 2.37 mm) than in the latter (8.07 ± 2.42 mm) group, but the difference was not statistically significant ($p=0.121$; Figure 3). Interobserver variability was $12.8 \pm 10.1\%$ and intraobserver variability was $4.7 \pm 4.1\%$ for the Doppler measurement data. 10 patients who received endoscopic treatments before B-RTO were treated by initial B-RTO alone. There was no significant difference between the therapeutic effect of B-RTO and clinical backgrounds such as bleeding history, presence of HCC or Child–Pugh classification.

Discussion

The management of bleeding GV is critical in the clinical practice of patients with portal hypertension [1–5]. Recent developments in medical technologies have resulted in the improvement of therapeutic outcome in patients with GV, and the greater application of B-RTO may be the most noteworthy advancement [6–10].

As shown by our results, GV were completely embolised in 30/34 patients (88.2%): 27 patients by initial 1-h B-RTO and 3 patients by a second 1-h B-RTO, which is similar to results from previous studies [6, 8–10]. In addition, there were neither serious complications nor recurrent cases during the observation period. Although 1 h was thought to be a time that patients could easily tolerate in the supine position under local anaesthesia alone, it is true that this selection of procedure duration was not based on scientific evidence. However, as our method could achieve sufficient therapeutic effect in the majority of patients with moderate- or large-grade GV, the results from this study might help the standardisation of the B-RTO method. Additionally, the optimum occlusion time to achieve complete embolisation should be examined in cases with a highly developed SGV before B-RTO as a tailor-made treatment.

A single session of 1 h B-RTO did not provide complete embolisation in 7/34 (20.6%) of the GV patients. Flow velocity and flow volume in the SGV were significantly higher in these treatment-resistive cases than in cases completely treated after a single session. Meanwhile, there was no significant difference between the results of embolisation of GV and the clinical backgrounds, such as bleeding history, presence of HCC and degree of liver damage. Therefore, it is suggested that the therapeutic effect of 1 h B-RTO may depend on the pre-treatment haemodynamics of the SGV, a major inflow route for GV. Indeed, all 10 patients who received endoscopic treatment before B-RTO had complete embolisation of their GV after a single session; this might be caused by decreased blood flow in the SGV as a result of the endoscopic treatments prior to B-RTO. Although the SGV in such patients had treatment-modified haemodynamics before B-RTO, candidates for B-RTO of GV may include a certain number of these patients in clinical practice. As the purpose of our study was to examine the relationship between the therapeutic effect of B-RTO and haemodynamics in the SGV before

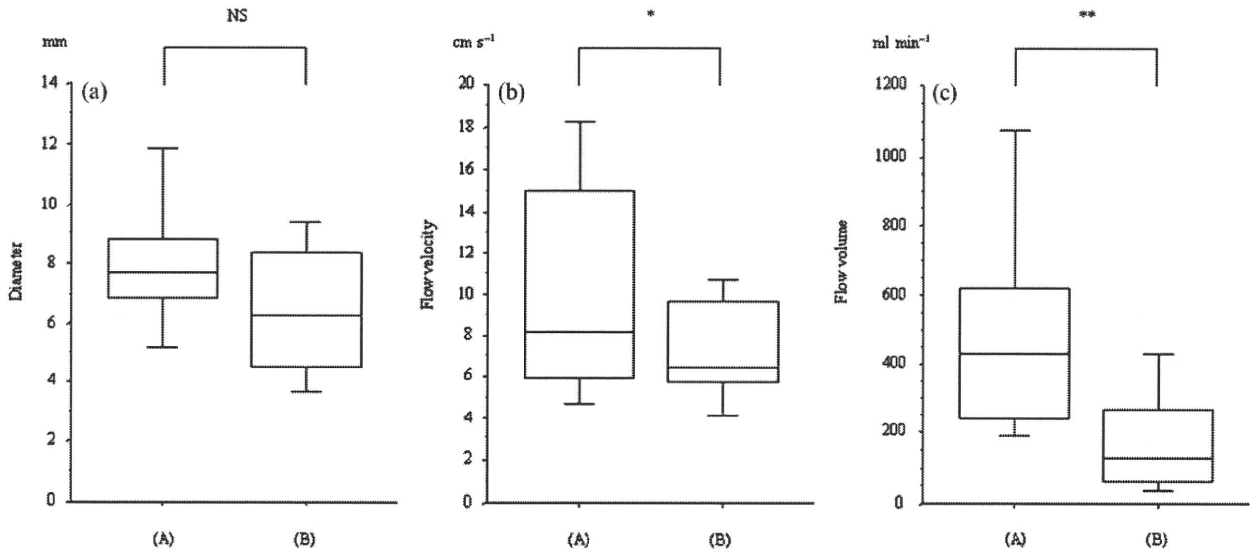

Figure 3. Relationship between the effect of balloon-occluded retrograde transvenous obliteration (B-RTO) and the haemodynamics of the short gastric vein (SGV) before treatment: (a) diameter, (b) flow velocity and (c) flow volume. (A) Patients incompletely treated by the initial B-RTO (n=7); and (B) patients completely treated by the initial B-RTO (n=27). Flow velocity and flow volume in the SGV before B-RTO were significantly lower in the 27 patients completely treated by initial B-RTO than in the 7 patients incompletely treated by initial B-RTO. Data were expressed by box-and-whisker plots. The top and bottom of the box indicate upper and lower quartiles, respectively, and the horizontal line in the box represents the median value. The two horizontal lines outside the box (whisker) indicates the smallest and largest non-outlier observation. *,** $p< 0.05$ (Student's t-test). NS, not significant.

B-RTO, the presence or absence of precedent endoscopic treatment might be trivial. Nevertheless, the evaluation of haemodynamics in the SGV by Doppler ultrasound before B-RTO may be predictive for the embolisation of GV.

There are few studies on the ultrasound findings of SGVs in the literature. The previous work reported a poor detectability of 10%, which may be caused by low performance of ultrasound equipment 20 years ago and/or the study subjects with portal hypertension not being limited to patients with moderate- or large-grade GV, as in our study [12]. Meanwhile, the SGV was detected and the blood flow was measured by ultrasound in 60.7% patients who had a SGV on the venogram in our study. Nowadays, Doppler ultrasound could be one of the tools used to assess the haemodynamics in the SGV that might reflect the pathophysiology of patients with GV.

Endoscopic cyanoacrylate injection is effective for the treatment of bleeding gastric varices. However, it does not necessarily provide sufficient long-term protection against GV bleeding, and previous reports have shown a cumulative rebleeding rate from 18–33% per year after cyanoacrylate injection [17, 18]. Therefore, the application of endoscopic treatment alone as a curative treatment for bleeding GV may be insufficient, and subsequent additional treatment, such as B-RTO, may be required. An appropriate timing of elective B-RTO after the haemostasis by endoscopic treatment should be established in the near future.

There were some limitations to our study. The first is that the therapeutic effect of B-RTO in the present study was compared with the haemodynamics in the SGV alone. As other collateral vessels, such as the LGV and/or PGV, are also inflow routes into GV in some cases [11], the haemodynamics of these vessels might be involved with the therapeutic effect of B-RTO. The next is that our data lack values of portal venous pressure, which might be associated with the embolisation effect of GV. Although the previous study has shown that portal venous pressure is not always high in patients with GV owing to the development of a gastrorenal shunt [11], B-RTO increases the portal venous pressure by embolisation of the variceal route [19]. The relationship between portal venous pressure and the therapeutic effect of B-RTO remains to be solved in further studies. Thirdly, our results were obtained in a retrospective study. The embolisation effect of B-RTO needs to be confirmed according to the haemodynamics in the SGV on Doppler ultrasound in prospective studies with large number of patients.

In conclusion, 1 h B-RTO may be a promising treatment method for moderate- to large-grade GV and could provide sufficient embolisation. Pre-treatment evaluation of portal haemodynamics by Doppler ultrasound might be predictive for the therapeutic effect of this technique.

References

1. Sarin SK, Sachdev G, Nanda R, Misra SP, Broor SL. Endoscopic sclerotherapy in the treatment of gastric varices. Br J Surg 1988;75:747–50.
2. Sarin SK, Lahoti D, Saxena SP, Murthy NS, Makwana UK. Prevalence, classification and natural history of gastric varices: a long-term follow-up study in 568 portal hypertension patients. Hepatology 1992;16:1343–9.
3. Kim T, Shijo H, Kokawa H, Tokumitsu H, Kumara K, Ota K, et al. Risk factors for hemorrhage from gastric fundal varices. Hepatology 1997;25:307–12.
4. Trudeau W, Prindiville T. Endoscopic injection sclerosis in bleeding gastric varices. Gastrointest Endosc 1986;32:264–8.

5. Akiyoshi N, Shijo H, Iida T, Yokoyama M, Kim T, Ota K, et al. The natural history and prognostic factors in patients with cirrhosis and gastric fundal varices without prior bleeding. Hepatol Res 2000;17:145–55.
6. Kanagawa H, Mima S, Kouyama H, Gotoh K, Uchida T, Okuda K. Treatment of gastric fundal varices by balloon occluded retrograde transvenous obliteration. J Gastroenterol Hepatol 1996;11:51–8.
7. Koito K, Namieno T, Nagakawa T, Morita K. Balloon-occluded retrograde transvenous obliteration for gastric varices with gastrorenal or gastrocaval collaterals. AJR Am J Roentgenol 1996;167:1317–20.
8. Hirota S, Matsumoto S, Tomita M, Sako M, Kono M. Retrograde transvenous obliteration of gastric varices. Radiology 1999;211:349–56.
9. Chikamori F, Kuniyoshi N, Shibuya S, Takase Y. Eight years of experience with transjugular retrograde obliteration for gastric varices with gastrorenal shunt. Surgery. 2001;129:414–20.
10. Fukuda T, Hirota S, Sugimura K. Long-time results of balloon-occluded retrograde transvenous obliteration for the treatment of gastric varices and hepatic encephalopathy. J Vasc Interv Radiol 2001;12:327–36.
11. Watanabe K, Kimura K, Matsutani S, Ohto M, Okuda K. Portal hemodynamics in patients with gastric varices: a study of 230 patients with esophageal and gastric varices using portal vein catheterization. Gastroenterology 1988;95:434–40.
12. Dokmeci AK, Kimura K, Matsutani S, Ohto M, Ono T, Tsuchiya Y, et al. Collateral veins in portal hypertension: demonstration by sonography. AJR Am J Roentgenol 1981;137:1173–8.
13. Matsutani S, Furuse J, Ishii H, Mizumoto H, Kimura K, Ohto M. Hemodynamics of the left gastric vein in portal hypertension. Gastroenterology 1993;105:513–8.
14. Pugh RN, Murray-Lyon IM, Dawson JL, Pietroni MC, Williams R. Transection of oesophagus for bleeding oesophageal varices. Br J Surg 1973;60:646–9.
15. The general rules for study of portal hypertension. 2nd edn. The Japan Society for Portal Hypertension. Tokyo: Kanehara, 2004:51–9.
16. Maruyama H, Okugawa H, Yoshizumi H, Kobayashi S, Yokosuka O. Hemodynamic features of gastrorenal shunt: a Doppler study in cirrhotic patients with gastric fundal varices. Acad Radiol 2008;15:1148–54.
17. Sarin SK, Jain AK, Jain M, Gupta R. A randomized controlled trial of cyanoacrylate versus alcohol injection in patients with isolated fundic varices. Am J Gastroenterol 2002;97:1010–5.
18. Akahoshi T, Hashizume M, Shimabukuro R, Tanoue K, Tomikawa M, Okita K, et al. Long-term results of endoscopic histoacryl injection sclerotherapy for gastric variceal bleeding. A 10-year experience. Surgery 2002;131:S176–81.
19. Akahane T, Iwasaki T, Kobayashi N, Tanabe N, Takahashi N, Gama H, et al. Changes in liver function parameters after occlusion of gastrorenal shunt with balloon-occluded retrograde transvenous obliteration. Am J Gastroenterol 1997;92: 1026–30.

Human Pathology (2009) 40, 1304–1311

ELSEVIER

Human
PATHOLOGY

www.elsevier.com/locate/humpath

Original contribution

Distinct expression of polycomb group proteins EZH2 and BMI1 in hepatocellular carcinoma

Yutaka Yonemitsu[a], Fumio Imazeki[a], Tetsuhiro Chiba[b], Kenichi Fukai[a], Yuichiro Nagai[c], Satoru Miyagi[b], Makoto Arai[a], Ryutaro Aoki[a], Masaru Miyazaki[d], Yukio Nakatani[e], Atsushi Iwama[b], Osamu Yokosuka[a,*]

[a]*Department of Medicine and Clinical Oncology, Graduate School of Medicine, Chiba University, Chiba 260-8670, Japan*
[b]*Department of Cellular and Molecular Medicine, Graduate School of Medicine, Chiba University, Chiba 260-8670, Japan*
[c]*Department of Molecular Pathology, Graduate School of Medicine, Chiba University, Chiba 260-8670, Japan*
[d]*Department of General Surgery, Graduate School of Medicine, Chiba University, Chiba 260-8670, Japan*
[e]*Department of Basic Pathology, Graduate School of Medicine, Chiba University, Chiba 260-8670, Japan*

Received 2 August 2008; revised 20 January 2009; accepted 30 January 2009

Keywords:
EZH2;
BMI1;
Hepatocellular carcinoma;
Short hairpin RNA;
MTS assay

Summary Polycomb gene products play a crucial role in the development of highly malignant phenotypes and aggressive cancer progression in a variety of cancers; however, their role in hepatocellular carcinoma remains unclear. First, we analyzed the impact of EZH2 and BMI1 modulation on cell growth of HepG2 cells. 3-(4,5-Dimethylthiazol-2-yl)-5-(3-carboxymethoxyphenyl)-2-(4-sulfophenyl)-2*H*-tetrazolium assays revealed marked growth inhibition after *EZH2* or *BMI1* knockdown. In addition, simultaneous knockdown of these 2 genes further augmented cell growth inhibitory effects. Next, we conducted immnuohistochemical assessment of 86 hepatocellular carcinoma surgical specimens, evaluating the correlation between EZH2 and BMI1 protein expression and clinicopathologic features. High-level EZH2 and BMI1 expression was detected in 57 (66.3%) and 52 tumor tissues (60.5%), respectively. Among these, 48 tumor tissues (55.8%) showed colocalization of EZH2 and BMI1 in almost all tumor cells. The cumulative recurrence rate, but not survival rate, was significantly higher in patients positive for EZH2 ($P = .029$) and BMI1 ($P = .039$) than in their negative counterparts, as determined by Kaplan-Meier analysis. These data indicate that EZH2 and BMI1 may cooperate in initiation and progression of hepatocellular carcinoma.

1. Introduction

Cell-type–specific gene expression profiles are stabilized by changes in chromatin structure and DNA methylation patterns. Polycomb group proteins form multiprotein complexes and serve as a cellular memory system through epigenetic chromatin modifications [1,2]. So far, 2 major polycomb group complexes have been well characterized. Polycomb repressive complex 1 includes BMI1, RNF110/MEL18, HPH, CBX2/HPC1, Ring1A, and Rind1B, and polycomb repressive complex 2 includes EED, EZH2, and SUZ12. The polycomb repressive complex 1 and polycomb repressive complex 2 possess H2A-K119 ubiquitin E3 ligase activity and H3-K27 methyltransferase activity, respectively. BMI1, which is part of the polycomb repressive complex 1, contributes to the enhancement of RING1-mediated H2A-K119 ubiquitin E3 ligase activity. EZH2, a key molecule of

* Corresponding author.
E-mail address: yokosukao@faculty.chiba-u.jp (O. Yokosuka).

0046-8177/$ – see front matter © 2009 Elsevier Inc. All rights reserved.
doi:10.1016/j.humpath.2009.01.017

polycomb repressive complex 2, possesses histone methyltransferase activity and causes methylation at lysine residues of histone H3 (H3-K27). Both histone modifications contribute to polycomb group gene silencing. Although no physical associations have been demonstrated between the 2 complexes, H3-K27 methylation serves as a binding site for the recruitment of the polycomb repressive complex 1. Thus, the 2 polycomb group complexes could function in a cooperative manner to maintain gene silencing [1,2].

Polycomb repressive complex 1 has been implicated in stem cell self-renewal [1,2], a process by which epigenetic cellular memory is precisely inherited by daughter cells through cell division. Among polycomb repressive complex 1 components, we have demonstrated that BMI1 plays a central role in the inheritance of self-renewal of hematopoietic stem cells in both loss-of-function and gain-of-function analyses [3]. It is well recognized that polycomb repressive complex 1 transcriptionally represses tumor suppressor genes such as the Ink4b-Arf-Ink4a locus, which functions as a barrier to eliminate oncogenic cells by triggering apoptosis or cellular senescence [1,4]. We have demonstrated that tight repression of Ink4a-Arf in hematopoietic stem cells is essential to maintain the self-renewing capacity of hematopoietic stem cells [5]. On the other hand, there is increasing evidence that up-regulation of polycomb group proteins is deeply involved in tumor development. EZH2 is reportedly involved in the pathogenesis of malignant lymphoma and multiple myeloma [6,7]. BMI1 was initially identified as a c-myc–cooperating protooncogene in murine lymphomas [8], and increased levels of BMI1 expression has been implicated not only in human lymphoma but also in several types of leukemia [9-11]. Moreover, coexpression of EZH2 and BMI1 appears to be associated with the degree of malignancy in B-cell non–Hodgkin lymphoma [12]. Of importance, recent studies demonstrated that the increased expression of EZH2 proteins correlates with progression and poor prognosis of solid tumors such as prostate cancer and breast cancer [13-15].

In the present study, we first examined the cell growth activity of hepatocellular carcinoma cells stably expressing short hairpin RNAs against EZH2 and BMI1 in culture. Next, we conducted immunohistochemical analyses to estimate the expression levels of polycomb group proteins EZH2 and BMI1 in hepatocellular carcinoma. The cumulative survival rates and recurrent rates were analyzed using the Kaplan-Meier method to ask whether these molecules could be novel biologic markers.

2. Materials and methods

2.1. Cell culture

The hepatocellular carcinoma cell line HepG2 was cultured in Dulbecco's modified Eagle's medium (Invitrogen Life Technologies, Carlsbad, CA) supplemented with 10% fetal bovine serum and 1% penicillin/streptomycin (Invitrogen).

2.2. Lentiviral production and transduction

Lentiviral vectors (CS-H1-short hairpin RNA EF-1α-EGFP and CS-CDF-RfA-ERP) expressing short hairpin RNA that targets human EZH2 (target sequence: 5′-GGAAAGAACGGAAATCTTA-3′), human BMI1 (target sequence: 5′-GAGAAGGAATGGTCCACTT-3′), and luciferase were constructed. Recombinant lentiviruses were produced as described elsewhere [3]. The cells were transduced with viruses in the presence of protamine sulfate.

2.3. Immunocytochemical analyses

HepG2 cells were fixed with methanol. After blocking in 10% goat serum, the cells were stained with a primary rabbit anti-EZH2 antibody (Zymed, San Francisco, CA) and a primary mouse anti-BMI1 antibody (Upstate Biotechnology, Lake Placid, NY) for 12 hours at 4°C. The cells then were washed and incubated with Alexa-555–conjugated goat anti-rabbit immunoglobulin G (IgG) (Molecular Probes, Eugene, OR) or Alexa-488–conjugated goat anti-mouse IgG (Molecular Probes), as appropriate, for 2 hours at room temperature. After being washed in phosphate-buffered saline (PBS), the cells were coverslipped with a mounting medium containing 4′,6-diamidino-2-phenylindole (DAPI) dihydrochloride (Vector Laboratories, Burlingame, CA).

2.4. Measurement of cell proliferation by 3-(4,5-dimethylthiazol-2-yl)-5-(3-carboxymethoxyphenyl)-2-(4-sulfophenyl)-2H-tetrazolium assay

Cell growth of HepG2 cells after stable knockdown of EZH2 and/or BMI1 was measured by 3-(4,5-dimethylthiazol-2-yl)-5-(3-carboxymethoxyphenyl)-2-(4-sulfophenyl)-2H-tetrazolium (MTS) assay. For this, we seeded cells in a 6-well plate at a density of 1×10^4 cells per well. MTS assays were performed in triplicate using the Cell Titer 96 Aqueous One Solution Cell Proliferation kit (Promega, Madison, WI) at culture days 2, 3, 4, and 5.

2.5. Patients and surgical specimens

Eighty-six patients who underwent surgical resection for hepatocellular carcinoma at Chiba University, Chiba, Japan, hospital were analyzed in this study. Informed consent for research use of the specimens was obtained for all cases. There were 73 male patients and 13 female patients with an average age of 63 ± 11 years (52-80 years). Among these, 32 cases had liver cirrhosis and 50 cases showed chronic hepatitis with mild to moderate activities. Liver damage of the patients was due to autoimmune disorder (n = 1), hepatitis B virus (HBV) (n = 19), hepatitis C virus (HCV)

(n = 38), both HBV and HCV (n = 2), and unknown etiology (n = 26). Paraffin-embedded sections of the tumors and surrounding nontumor liver tissues were examined by hematoxylin-eosin (H&E) staining and immunohistochemistry.

2.6. Immunohistochemical analyses

After deparaffinization and inhibition of endogenous peroxidase activities, the pathologic specimens of surgically resected tumors were stained with rabbit anti-EZH2 (1:100, Zymed), mouse anti-BMI1 (1:100, Upstate Biotechnology) or mouse anti–Ki-67 (1:50; Santa Cruz Biotechnology, Santa Cruz, CA) antibodies. Before incubation with the primary antibodies, antigen retrieval was performed with ethylenediaminetetraacetic acid buffer (pH 8.0) in a pressure cooker at 100°C for 1 minute. The proteins were detected using ImmPRESS peroxidase micropolymer staining kits (Vector Laboratories) and 3,3′-diaminobenzidine substrate according to the manufacturer's instructions. To investigate the colocalization of EZH2 and BMI1, we simultaneously stained the clinical specimens with indicated antibodies. Subsequently, they were stained with Alexa-555–conjugated goat anti-rabbit IgG (Molecular Probes) and Alexa-488–conjugated goat anti-mouse IgG (Molecular Probes), respectively.

2.7. Statistical analyses

Statistical differences between 2 groups in MTS assays were analyzed using the Student t test. The correlations between the expression of polycomb group proteins and clinicopathologic features were assessed using the χ^2 test and Student t test to analyze qualitative and quantitative data, respectively. The cumulative survival and recurrent rates were analyzed by the Kaplan-Meier method, and the statistical significance between the 2 groups positive and

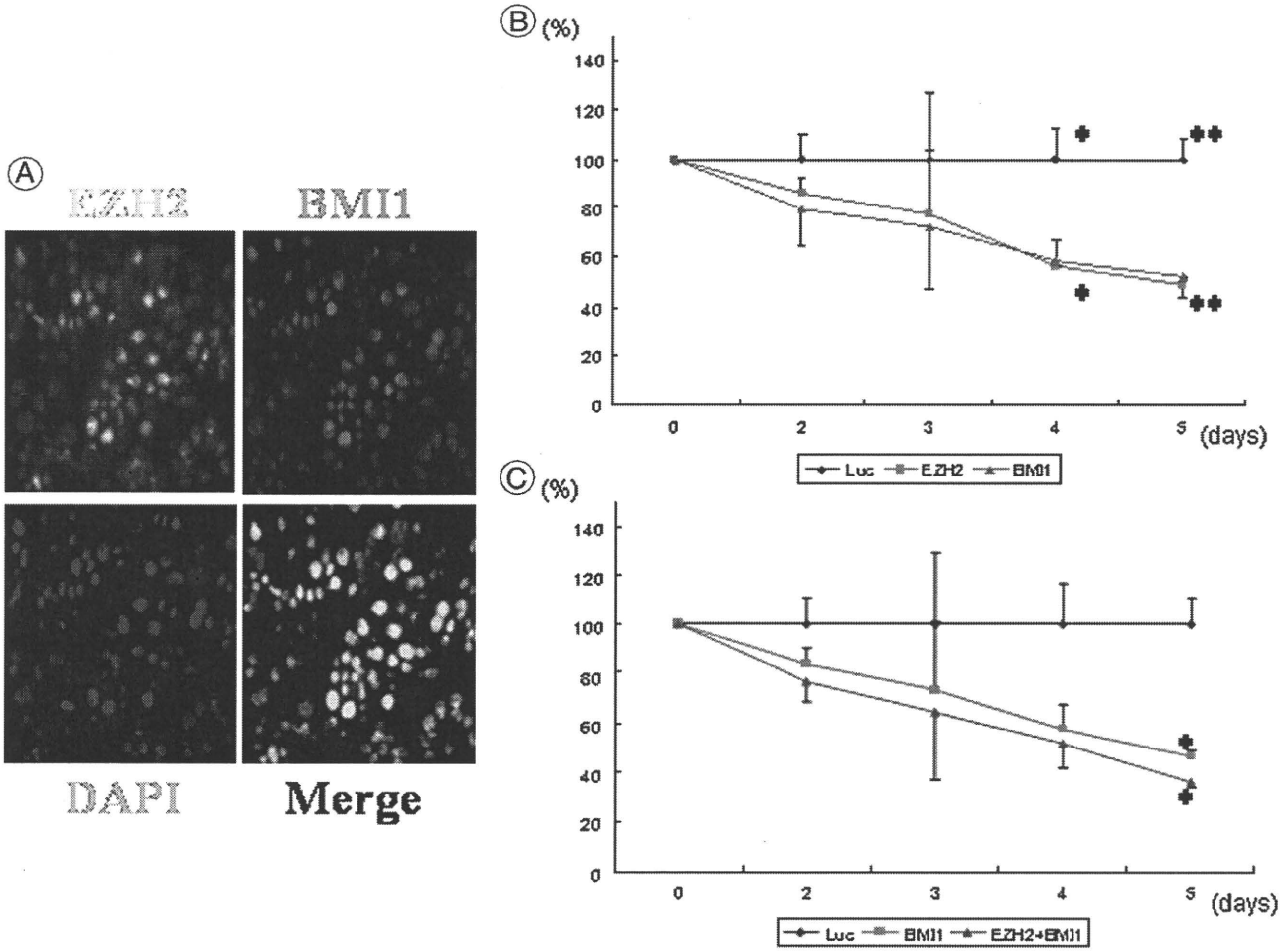

Fig. 1 Loss-of-function assays of EZH2 and BMI1 in HepG2 cells. (A) Immunocytochemical analyses of EZH2 and BMI1. Immunofluorescent labeling of EZH2 (green), BMI1 (red), and nuclear DAPI staining (blue) is merged. (B) Cell growth inhibition of EZH2 or BMI1 knockdown HepG2 cells compared with luciferase knockdown HepG2 cells as a control. Mean ± SD values are shown for each group, $*P < .05$, $**P < .005$. (C) Augmented growth inhibition of both EZH2 and BMI1 knockdown HepG2 cells. Mean ± SD values are shown for each group, $*P < .005$.

negative for polycomb group immunostaining was analyzed using the Wilcoxon test. Cox proportional regression analysis was performed to estimate rate ratios for the effect of EZH2 and BMI1 staining in tumors for recurrence. Potential risk factors assessed for recurrence included the following variables: BMI1 in tumors (presence versus absence), EZH2 in tumors (presence versus absence), sex (male versus female), age (>65 versus ≤65 years), size of tumors (>45 versus ≤45 mm), differentiation (poorly versus well, moderately), TNM stage [16] (I + II versus III + IVa), protein induced by vitamin K absence II (PIVKA II) level (>100 versus ≤100 mAU/mL), α-fetoprotein (AFP) level (>40 versus ≤40 mg/mL), etiology (HBV and HCV versus HBV alone, HCV alone, non-HBV, and non-HCV), chronic hepatitis (versus liver cirrhosis), aspartate aminotransferase (AST) level (>50 versus ≤50 IU/L), alanine aminotransferase (ALT) level (>50 versus ≤50 IU/L), total bilirubin level (>1.0 versus ≤1.0 mg/dL), albumin level (>3.8 versus ≤3.8 g/dL), platelet count (>15 × 10^9/L versus ≤15 × 10^9/L), prothrombin time (>80% versus ≤80%), the presence of portal invasion (versus no portal invasion), and tumor number (>2 versus ≤2). Variables statistically significant by univariate Cox proportional regression analysis were further studied by multivariate analysis. The differences were considered significant at $P < .05$.

3. Results

3.1. Stable short hairpin RNA-mediated knockdown of EZH2 and BMI1 mediated growth inhibition in HepG2 cells

To examine the basal expression of EZH2 and BMI1 in hepatocellular carcinoma cells, we conducted dual immunocytochemical analyses in HepG2 cells. EZH2 and BMI1 were widely detected in the nucleus and were coexpressed in more than 70% of HepG2 cells (Fig. 1A). To gain insight into the role of the polycomb gene products in HepG2 cells, we performed loss-of-function assays using lentivirus-mediated knockdown techniques. MTS assays showed that cell growth activity was consistently repressed, after EZH2 and BMI1 knockdown, for the 5 days of the observation period (Fig. 1B). Cell growth activity at days 2, 3, 4, and 5 was 86% ± 6.2%, 77% ± 27%, 56% ± 10%, and 49% ± 2.4%, respectively, after EZH2 knockdown and 79% ± 15%, 72% ± 25%, 58% ± 2.5%, and 52% ± 8.3%, respectively, after BMI1 knockdown compared with the luciferase knockdown cells, with there being a statistically significant difference at day 4 ($P < .05$) and 5 ($P < .005$) in the case of EZH2 or BMI1 knockdown. Intriguingly, simultaneous knockdown of EZH2 and BMI1 mediated an even greater degree of growth inhibition of HepG2 cells (Fig. 1C). Cell growth activity at days 2, 3, 4, and 5 was 77% ± 7.9%, 65% ± 27%, 52% ± 10%, and 36% ± 1.8%, respectively, after simultaneous knockdown compared with luciferase knockdown cells, with there being a statistically significant difference at day 5 ($P < .005$) between knockdown of both EZH2 and BMI1 and that of BMI1 alone.

Table 1 EZH2 and BMI1 expression in hepatocellular carcinoma and equivalent nontumor tissues

	Tumor	Nontumor
EZH2	57/86 (66.3%)*	5/86 (5.8%)*
BMI1	52/86 (60.5%)**	4/86 (4.7%)**

*, **$P < .05$.

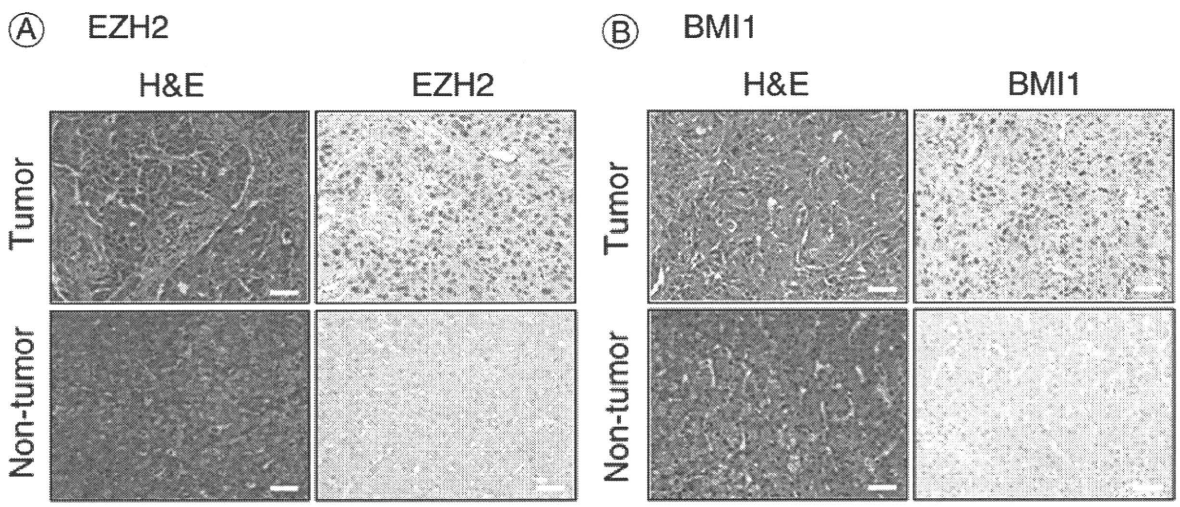

Fig. 2 Representative histopathologic analyses of EZH2 and BMI1. (A) H&E staining and immunohistochemical analysis of EZH2 in hepatocellular carcinoma tissue and the corresponding nontumor tissue. (B) H&E staining and immunohistochemical analysis of BMI1 in hepatocellular carcinoma tissue and the corresponding nontumor tissue (scale bar = 50 μm).

Table 2 The expression pattern of EZH2 and BMI1 in tumor and nontumor tissues

	Tumor				Nontumor			
	BMI1+	BMI1−	Total	*P*	BMI1+	BMI1−	Total	*P*
EZH2+	48	9	57	<.01	0	5	5	>.99
EZH2−	3	26	29		4	77	81	
Total	51	35	86		4	82	86	

3.2. Preferential expression of EZH2 and BMI1 in hepatocellular carcinoma samples

We evaluated the expression levels of polycomb group proteins EZH2 and BMI1 in hepatocellular carcinoma tissues and the corresponding nontumor tissues obtained from 86 patients by histopathologic analyses. Representative immunohistochemical staining of EZH2 and BMI1 is shown in Fig. 2A and B. The expression of EZH2 and BMI1 was diffusely detected in the nuclei of cancer cells, and no patients showed focal expression of these proteins in tumor tissues.

Fifty-seven (66.3%) of 86 hepatocellular carcinoma samples were positive for EZH2, whereas only 5 (5.8%) of 86 nontumor samples showed EZH2 expression ($P < .01$) (Table 1). On the other hand, BMI1 expression was detected in 52 (60.5%) of 86 hepatocellular carcinoma samples, whereas its expression was detected in only 4 (4.7%) of 86 nontumor samples ($P < .01$) (Table 1). Of importance, 48 (55.8%) of 86 hepatocellular carcinoma samples expressed both EZH2 and BMI1 (Table 2). Consequently, 26 (30.2%) of 86 samples did not express either protein. These results showed a statistically significant difference with respect to EZH2-positive ratio between BMI1-positive and BMI1-negative tumor tissues ($P < .01$). In contrast, 77 (89.5%) of 86 nontumor samples were negative for both EZH2 and BMI1 (Table 2). These results indicate that the expression of EZH2 and BMI1 is preferentially up-regulated in hepatocellular carcinoma samples, and their expression patterns could segregate hepatocellular carcinoma samples into subgroups.

3.3. Coexpression of EZH2 and BMI1 in hepatocellular carcinoma tissues

To determine whether EZH2 and BMI1 are coexpressed in the same hepatocellular carcinoma cells, we performed dual immunofluorescence staining on 10 randomly selected hepatocellular carcinoma tissues that were positive for both EZH2 and BMI1 by conventional immunohistochemical analysis. As shown in Fig. 3, EZH2 and BMI1 were detected in the nucleus and were coexpressed in more than 70% of hepatocellular carcinoma cells in all samples analyzed. These results strongly indicate cooperative contributions of EZH2 and BMI1 to the development and progression of hepatocellular carcinoma.

3.4. Correlation between the expression of EZH2 or BMI1 and that of Ki-67

We performed immunohistochemical analysis of Ki-67 in tumor and nontumor tissues and compared the results with those of EZH2 and BMI1 (Table 3). EZH2 was positive in 47 (80%) of 59 Ki-67–positive tumors and in 10 (37%) of 27 Ki-67–negative tumors ($P = .0002$). BMI1 was also positive in 44 (75%) of 59 Ki-67–positive tumors and in 8 (30%) of 27 Ki-67–negative tumors ($P = .0001$). In nontumor tissues, the staining of Ki-67 was found only in 11 cases, and we found no correlation between these 2 proteins and Ki-67 (Table 3).

3.5. Relationship between EZH2 or BMI1 expression and clinicopathologic features

We next evaluated the relationship between increased expression of polycomb group proteins and clinicopathologic parameters of the 86 hepatocellular carcinoma patients (Table 4). Significant correlation was observed between increased EZH2 expression in hepatocellular carcinoma tissues and hypoalbuminemia ($P = .01$) or advanced TNM stage ($P = .04$). In contrast, increased BMI1 expression in the

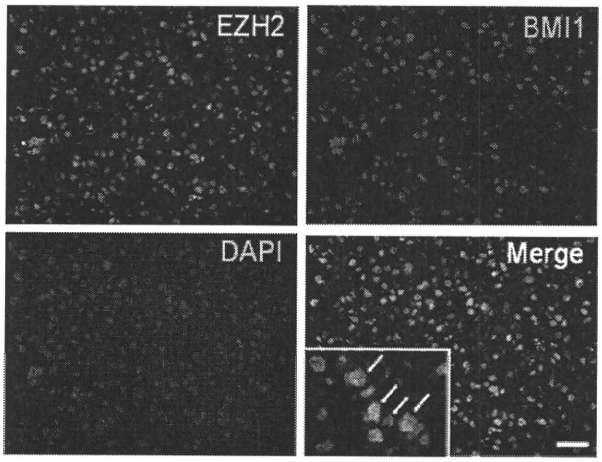

Fig. 3 Representative dual immunostaining of EZH2 (green) and BMI1 (red) in hepatocellular carcinoma tissue and the corresponding nontumor tissue. The nuclei were stained with DAPI (blue). Arrows indicate a typical nucleus positive for EZH2, BMI1, and DAPI (scale bar = 50 μm).

Table 3 Correlation between the expression of EZH2 or BMI1 and that of Ki-67

	Tumor				Nontumor			
	Ki-67+	Ki-67−	Total	*P*	Ki-67+	Ki-67−	Total	*P*
EZH2+	47	10	57	.0002	1	4	5	>.50
EZH2−	12	17	29		10	71	81	
Total	59	27	86		11	75	86	
BMI1+	44	8	52	.0001	1	3	4	.43
BMI1−	15	19	34		10	72	82	
Total	59	27	86		11	75	86	

hepatocellular carcinoma samples had no significant correlation with clinicopathologic factors.

3.6. Prognostic value of EZH2 or BMI1 expression in hepatocellular carcinoma patients

To elucidate the role of polycomb group proteins in hepatocellular carcinoma progression, we performed prognostic analyses of 61 hepatocellular carcinoma patients in whom curative operation was conducted and whose postoperative course could be followed. The cumulative recurrent rates and survival rates were analyzed by the Kaplan-Meier method (Fig. 4A-D). During the follow-up period (27.2 ± 19.6 months), 39 patients developed a recurrence of hepatocellular carcinoma and 19 patients died from relapsed hepatocellular carcinoma. Our results demonstrated higher cumulative recurrence rates in EZH2-positive patients than in EZH2-negative patients (P = .029). In contrast, the cumulative survival rates showed no significant differences between EZH2-positive and EZH2-negative patients. Of interest, results of the prognostic analysis correlating BMI1 expression were similar to those of the EZH2 expression-based analysis. The cumulative recurrence rates were higher in BMI1-positive patients than in BMI1-negative patients (P = .039), although the difference in survival rates between the 2 groups was not significant. Given that EZH2 and BMI1 are frequently coexpressed in the same samples, these prognostic findings appear quite reasonable.

Table 4 Correlation between polycomb group protein expression and clinicopathologic background in 86 hepatocellular carcinoma samples

Variables	EZH2 expression			BMI1 expression		
	Negative (n = 29)	Positive (n = 57)	*P*	Negative (n = 34)	Positive (n = 52)	*P*
Sex (male/female)	27/2	46/11	.13	31/3	42/10	.46
Age (y)	64.7 ± 9.8	62.6 ± 12.5	.45	63.6 ± 11.6	63.1 ± 11.8	.86
Liver function						
AST (IU/L)	66.8 ± 79.4	94.8 ± 126.0	.30	67.4 ± 75.0	97.2 ± 131.2	.25
ALT (IU/L)	71.4 ± 64.8	90.4 ± 122.3	.46	71.9 ± 64.3	92.0 ± 126.8	.42
Total bilirubin (mg/dL)	1.00 ± 0.38	1.12 ± 0.64	.39	0.96 ± 0.36	1.15 ± 0.66	.15
Albumin (g/dL)	4.02 ± 0.48	3.70 ± 0.53	.01[a]	3.92 ± 0.50	3.74 ± 0.55	.14
Prothrombin time (%)	84.4 ± 12.9	84.7 ± 19.3	.95	83.6 ± 12.5	85.1 ± 20.0	.76
Platelet ($\times 10^4$/mL)	15.60 ± 6.62	15.89 ± 6.66	.85	15.94 ± 6.88	15.70 ± 6.5	.88
PIVKA II (mAU/mL)	4027.0 ± 9934.8	5040.6 ± 12 873.8	.76	5654.6 ± 13 844.7	4250.1 ± 11 063.9	.65
AFP (mg/mL)	108.0 ± 181.6	9570.6 ± 37 690.7	.21	3710.9 ± 19 937.8	8283.1 ± 36 691.8	.53
Tumor factors						
Tumor size (mm)	47.4 ± 33.5	51.4 ± 33.6	.63	51.3 ± 34.5	49.4 ± 33.0	.81
No.	1.19 ± 0.51	1.40 ± 0.61	.18	1.26 ± 0.59	1.38 ± 0.58	.40
VP (+) (%)	3/19 (15.8%)	17/50 (34%)	.23	7/24 (29.2%)	13/45 (28.9%)	>.99
Well/moderate/poorly[b]	4/16/4	6/36/9	.84	5/20/4	5/32/9	.64
TNM (I/II/III/IVa)	5/15/4/0	5/25/20/8	.04[a]	4/17/8/0	6/23/16/8	.14
Etiology						
AIH/B/C/B and C/BC (−)	0/5/12/0/12	1/14/26/2/14	.63	1/6/14/0/13	0/13/24/2/13	.42
CH/LC	16/11	34/21	.81	21/11	29/21	.64

Abbreviations: VP, invasion to portal vein; AIH, autoimmune hepatitis; CH, chronic hepatitis; LC, liver cirrhosis; B, hepatitis B; C, hepatitis C.
NOTES: Reference range—AST, 10 to 35 IU/L; ALT, 5 to 40 IU/L; total bilirubin, 0.4 to 1.2 mg/dL; albumin, 3.9 to 5.2 g/dL; prothrombin time, 70% to 140%; platelet, 15 to 35 × 10^4/mL; PIVKA II, <40 mAU/mL; AFP, <20 ng/mL.
[a] Statistically significant.
[b] Histologic differentiation of the tumor.